LA-13274-M
Manual

FUGM Hardware Operation Manual

Los Alamos
NATIONAL LABORATORY
Los Alamos National Laboratory is operated by the University of California for the United States Department of Energy under contract W-7405-ENG-36.

Edited by Paul W. Henriksen, Group CIC-1.

Prepared by Celina M. Ortiz, Group NIS-5.

This work was supported by the Power Reactor and Nuclear Fuel Development Corporation of Japan in cooperation with the US Department of Energy, Office of Arms Control and Nonproliferation, International Safeguards Division.

An Affirmative Action/Equal Opportunity Employer

This report was prepared as an account of work sponsored by an agency of the United States Government. Neither The Regents of the University of California, the United States Government nor any agency thereof, nor any of their employees, makes any warranty, express or implied, or assumes any legal liability or responsibility for the accuracy, completeness, or usefulness of any information, apparatus, product, or process disclosed, or represents that its use would not infringe privately owned rights. Reference herein to any specific commercial product, process, or service by trade name, trademark, manufacturer, or otherwise, does not necessarily constitute or imply its endorsement, recommendation, or favoring by The Regents of the University of California, the United States Government, or any agency thereof. The views and opinions of authors expressed herein do not necessarily state or reflect those of The Regents of the University of California, the United States Government, or any agency thereof. Los Alamos National Laboratory strongly supports academic freedom and a researcher's right to publish; as an institution, however, the Laboratory does not endorse the viewpoint of a publication or guarantee its technical correctness.

LA-13274-M
Manual

UC-700
Issued: May 1997

FUGM Hardware Operation Manual

T. R. Wenz
H. O. Menlove
J. K. Halbig
S. F. Klosterbuer
J. Baca
K. Kroncke
J. McDow
T. Dye
M. Stephens
G. Wiig
R. Abedin-Zadeh*
P. Elomaa*
T. Iwamoto**
S. Ishi***

*International Atomic Energy Agency, Wagramerstrasse, Vienna, A-1200, AUSTRIA
**Power Reactor and Nuclear Fuel Development Corporation, Tokyo, JAPAN
***Japan Nuclear Safety Bureau, Science and Technology Agency, Tokyo, JAPAN

Los Alamos
NATIONAL LABORATORY
Los Alamos, New Mexico 87545

CONTENTS

FUGM HARDWARE OPERATION MANUAL

by

T. R. Wenz, H. O. Menlove, J. K. Halbig, S. F. Klosterbuer,
J. Baca, K. Kroncke, J. McDow, T. Dye, M. Stevens, G. Wiig,
R. Abedin-Zadeh, P. Elomaa, T. Iwamoto, and S. Ishi

ABSTRACT

This manual describes the detector design features, performance, and operating characteristics of the Fugen reactor gate monitor for monitoring fresh and spent fuel transfers between the core and storage ponds. This system consists of two monitors located at each end of the transfer chute. The larger monitor contains two ^{3}He tubes, two fission chambers, and two ion chambers. The smaller monitor, used for direction of motion redundancy, contains two ion chambers. All detectors provide information for identifying the type, fresh or spent UOX or MOX fuel, and direction of the fuel transfer. The gamma-ray and neutron detector (GRAND-3) electronics package supplies power to the radiation sensors and collects the radiation data for storage on a laptop computer. The system is designed to operate unattended with data collection by the inspectors occurring on 90-day time intervals. This manual also includes radiation data for the six types of fuel transfers and equipment transfers along with the direction of motion information collected during the installation at the Fugen reactor.

GENERAL

This manual describes the design features and operating characteristics of the Fugen gate monitor (FUGM) for fresh- and spent-fuel transfers. The FUGM will be used by the International Atomic Energy Agency (IAEA) and the Japanese National Inspectors to verify the time and direction of fresh and spent fuel movements through the transfer chute between the refueling pond inside the reactor containment and the spent fuel storage pool outside the reactor containment from the Fugen-prototype reactor.

The IAEA prepared the user requirements for the FUGM system and Los Alamos prepared the specifications and design of the integrated system including the detectors, electronics, computers, and software. The detector packages were installed on the fuel transfer chute by the IAEA in November 1995. The electronics and computers were also installed during this visit.

PHYSICAL DESCRIPTION

The FUGM system includes the following components:

- Large detector package under the transfer chute
  Two ion chambers (ICs)
  Two ^{3}He tubes
  Two fission chambers (FCs)
  Four PDT[a] preamplifiers
  Two remote disconnect relays
- Small detector package above the transfer chute
  Two ICs
  Two remote disconnect relays
- Electronics cabinet
- GRAND-3 (two each plus one spare)
  Two external battery backups
- Consultronics Linebacker computer (two each plus one spare)
- Bernoulli Transportable disk drive (two each)
- Uninterruptable power source, Smart UPS (two each)
- Power transformer (two each)

Figure 1 is a diagram of the large detector package illustrating the locations of the ion chambers, fission chambers, ^{3}He tubes, and PDT-110A preamplifiers. A more detailed diagram of the polyethylene piece that holds the neutron and gamma-ray detectors in the large detector package is shown in Fig. 2. The detectors are set in a

---

[a] Precision Data Technology, Inc., 6015 145th Street, SW, Edmunds, WA 98026

PHYSICAL DESCRIPTION
(cont.)

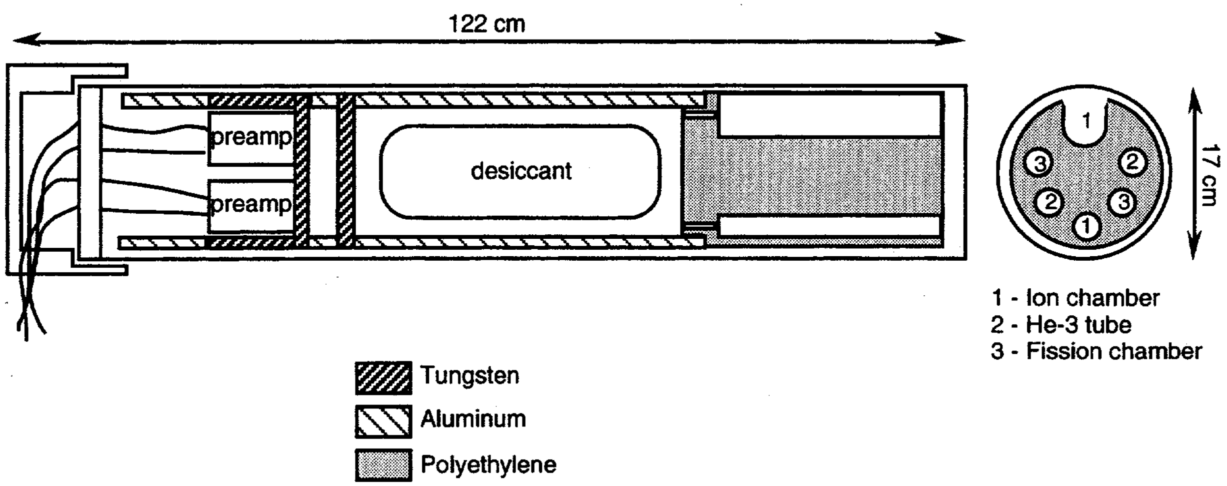

Fig. 1. Schematic diagram of the large FUGM detector package (A) located on the pool side of the transfer chute. The locations of the ^{3}He tubes, PDT preamplifiers, fission chambers, ion chambers, desiccant, and cable connections are illustrated.

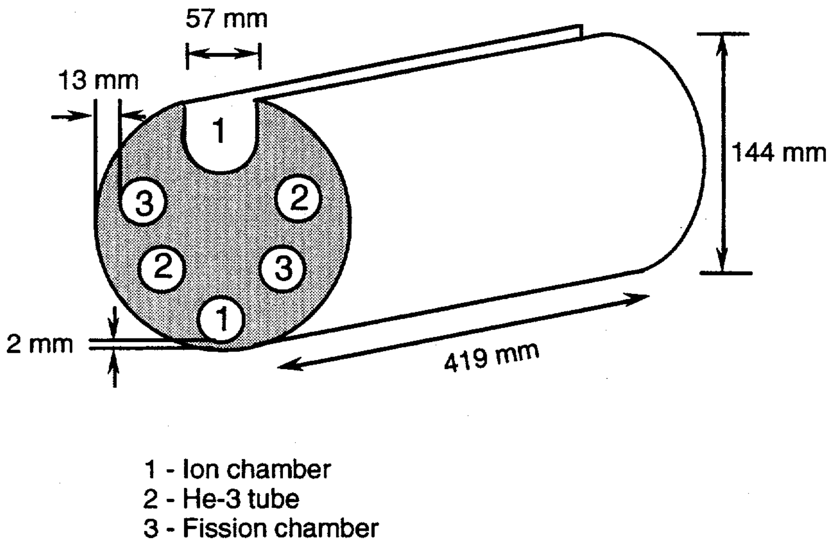

Fig. 2. Detailed drawing of the polyethylene insert that holds the fission chambers, ^{3}He tubes, and ion chambers in the large FUGM detector package.

polyethylene cylinder to fix their positions and to moderate the neutrons. The PDT preamplifiers are placed in an ~15-mm-thick tungsten shield to decrease the gamma-ray dose. Figure 3 is a diagram of the small detector package that contains ion chambers only. Figure 4 is a photograph of the large and small detector packages disassembled without the radiation detectors.

PHYSICAL DESCRIPTION
(cont.)

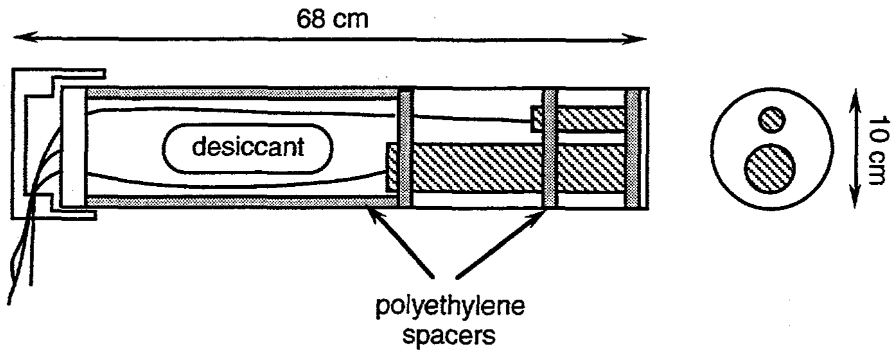

Fig. 3. Schematic diagram of the small FUGM detector package (B) located on the reactor side of the transfer chute. The locations of the large and small ion chambers, desiccant, and cable connections are illustrated.

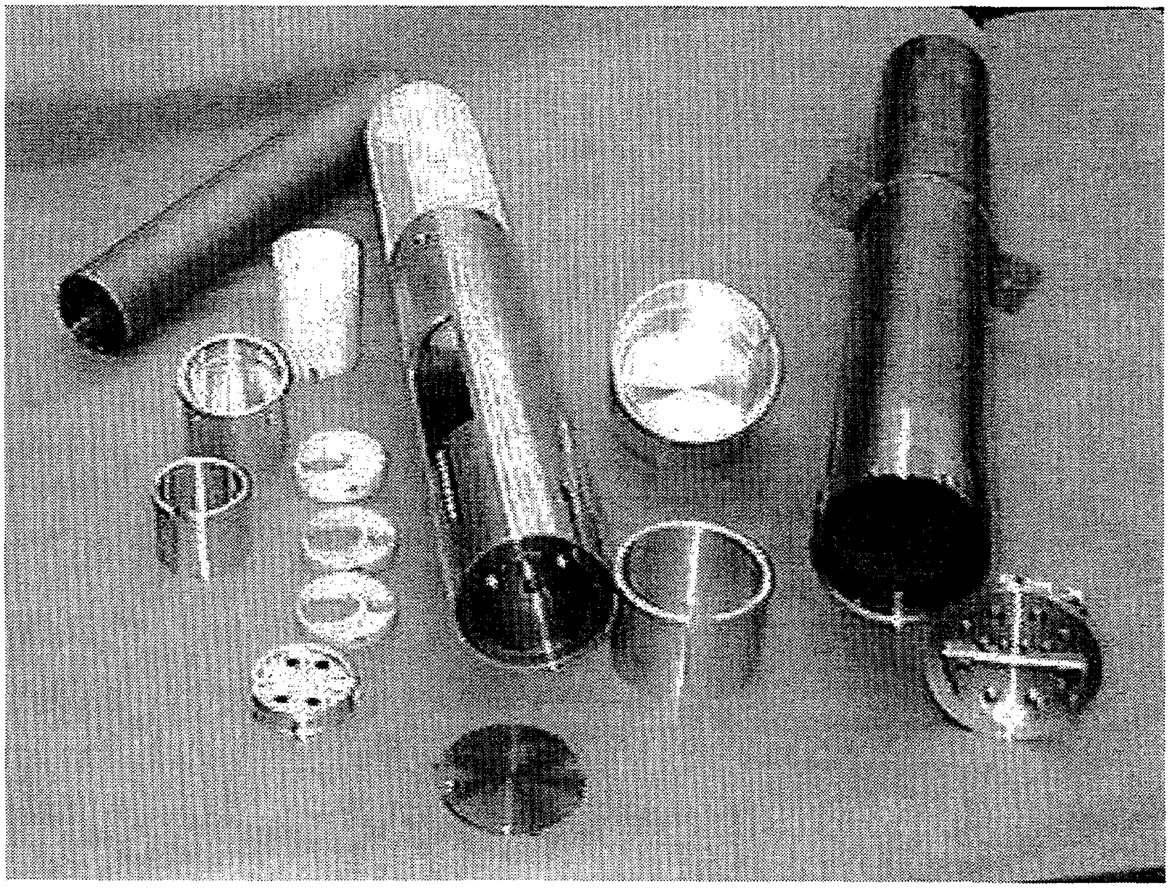

Fig. 4. Photograph of the components for the two FUGM detector packages showing the polyethylene and aluminum inserts that support the neutron and gamma-ray detectors and preamplifiers.

PHYSICAL DESCRIPTION (cont.)

The specifications for the ion chambers, ^{3}He tubes, and fission chambers are given in Table I. The units for the ion chamber sensitivity are Amps per Roentgen per hour.

TABLE I. Radiation Detector Specifications

Detector Type	Quantity	Operating Voltage (V)	Sensitivity
Ion chamber Model LND[b] 52110	2	-500	A/R/hr 3.4×10^{-10}
Ion chamber Model LND 50346	2	-500	A/R/hr 3.5×9^{-9}
^{3}He tube model RS-P4-0812-114[c]	2	1720	
Fission chamber Model RS-P6-0810-101	2	500	

The large detector package (A) is positioned ~60 cm from the center line of the fuel transfer chute, parallel to the reactor wall at the entrance to the spent fuel storage pool. The small detector package (B) is positioned horizontally in the transfer chute ~2 cm from the wall where the entrance to the reactor refueling pond is located. Figure 5 illustrates the placement of the detector packages relative to the transfer chute.

Both the ion chambers and ^{3}He tubes count gamma rays from the spent fuel as the fuel is pushed through the fuel transfer chute. The detectors are designed to measure gamma doses in the range of 0.01 to 10^{6} R/h. The actual dose at the detector is reduced because of the separation distance and the stainless steel shielding in the fuel transfer chute and from the outer housing of the detector assemblies.

Two fission chambers provide a very linear response to the neutron flux. Two ^{3}He tubes measure the neutron flux and provide a signal predominately based on the gamma-ray dose when the gamma dose rates in the vicinity of the detector exceed ~5-10 R/h. The ^{3}He tubes, however, are almost 100 times more sensitive to neutrons than are the fission chambers. The fission chambers are virtually immune to the gamma interference that can be experienced by the ^{3}He detectors.

---

[b] LND, Inc., 3230 Lawson Blvd., Oceanside, NY 11572

[c] GE Reuter-Stokes, Inc., 8499 Darrow Rd, Twinsburg, OH 44087

PHYSICAL DESCRIPTION (cont.)

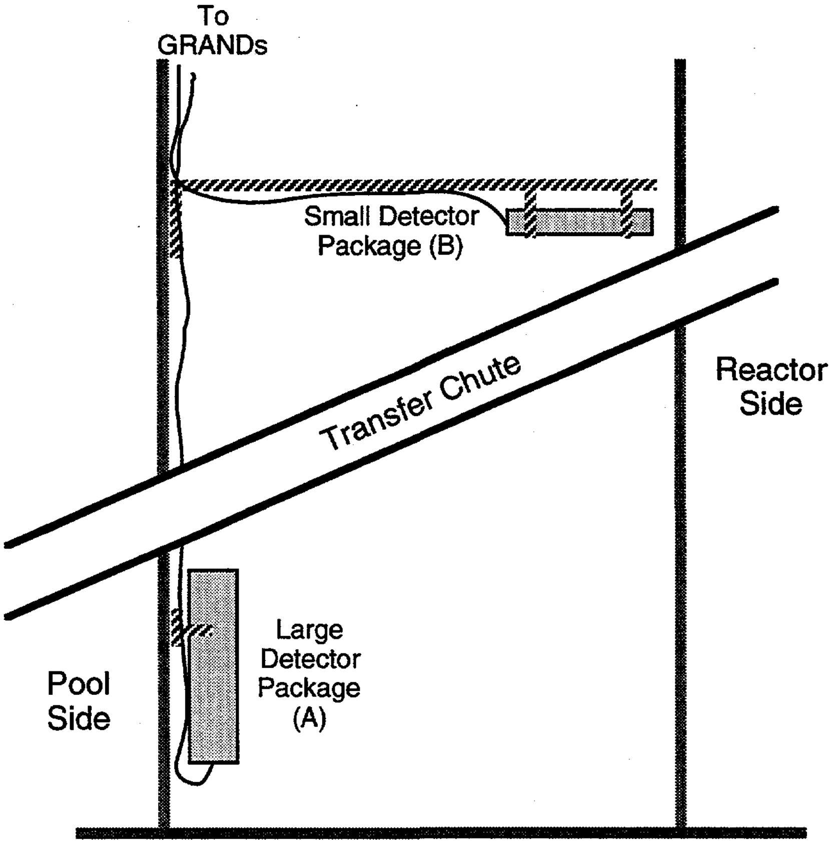

Fig. 5. Diagram of the reactor annulus shield area showing the positions of the large and small FUGM detector packages relative to the transfer chute.

Gamma radiation is measured primarily by two different pairs of ion chambers. The sensitivities of the ionization chambers differ by approximately a factor of 10. Both ionization chambers provide a linear range of approximately 0.01 to 106 R/h. The actual neutron and gamma-ray doses at the assemblies are attenuated at the detectors because the detectors are separated from the chute, and there is stainless steel in the fuel transfer chute and the outer housing of the detector enclosure. The water in the chute during transfer is a mild filter for the gamma rays, but does significantly reduce the neutron flux measured at the detectors.

ELECTRICAL CONNECTION

The GRANDs provide total logistical support for the detectors. The detector banks can be thought of as having more sensitive and less sensitive detectors. The more sensitive detectors, the large ICs and the ^{3}He tubes, are connected to one GRAND; the less sensitive detectors are

ELECTRICAL CONNECTION (cont.)

connected to the second GRAND. This is shown in Fig. 6. The two ^{3}He tubes and the two FCs are each connected to a PDT (Model 110A) preamplifier. In addition, one of the ^{3}He detectors and one of the fission chambers are cross-coupled to the other GRAND. Thus even if a GRAND or collect computer would fail, the pulse counting detectors associated with that GRAND would have representation via the other GRAND as long as power is still supplied by the failing GRAND.

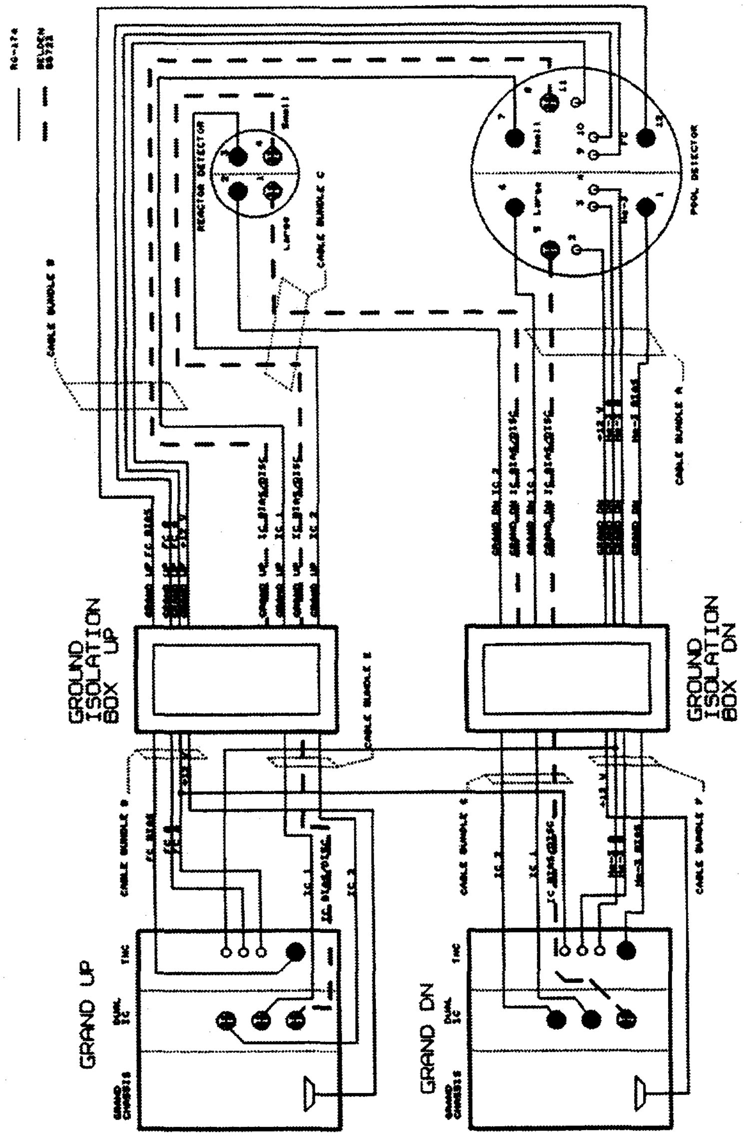

Fig. 6. Diagram of the component wiring in the FUGM electronics cabinet between the GRAND and the sensors in the large and small detector packages.

ELECTRICAL CONNECTION (cont.)

Approximately 70 m of cable connects the detectors and the electronics cabinet. To accommodate the long cable length, the PDT-110A was modified to operate at +12V (vs +5V) and the signal output logic pulse was lengthened to 200 ns (vs 50 ns).

A sealable electronics cabinet (76 cm x 61 cm x 183 cm) containing four shelves is used to house the equipment operating the gate monitor. Table II lists the components in the cabinet and Table III lists the shelf location of the components, along with the detectors the components operate.

TABLE II. FUGM Electronic Components

Primary Components	
Consultronics Linebacker 400 Computer	SN TM2099501227
Consultronics Linebacker 400 Computer	SN TM2099501231
Davidson GRAND-3	SN G3-083
Davidson GRAND-3	SN G3-084
Transportable 230 Bernoulli Disk Drive	SN MN15320170
Transportable 230 Bernoulli Disk Drive	SN MN15280090
Smart UPS SV700	SN S95025312699
Smart UPS SV700	SN S95025339999
Backup Components	
Consultronics	SN TM2099501229
GRAND-3	SN G3-085
Bernoulli	SN MN15320178

^{3}He-TUBE HIGH-VOLTAGE PLATEAU

The ^{3}He tubes are from Reuter-Stokes with a diameter of 25 mm and an active length of 305 mm. The fill-pressure of the tubes is four atmospheres of ^{3}He plus a nitrogen additive. The aluminum walls of the tube are coated with carbon for radiation resistance.

The high-voltage (hv) plateau for the FUGM ^{3}He tubes is shown in Fig. 7 where the totals counting rate from a ^{252}Cf source is plotted as a function of the hv bias applied to the detector tubes. The PDT-110A amplifier of tube A has higher gain than for tube B to provide different sensitivity levels for gamma-ray pileup interference. Thus, the ratio of tube A to tube B will be constant if there is no gamma-ray interference. We have set the high-voltage bias at 1720 V so that tube A will start to pick up gamma pileup counts above

^{3}He-TUBE HIGH-VOLTAGE PLATEAU

(cont.)

TABLE III. Location of Equipment in the FUGM Electronics Cabinet

Shelf No. (top-bottom)	Shelf Contents	Detectors Controlled by GRAND
Shelf 1	GRAND "UP" external battery pack	Pool-FC1 Pool-FC2 Pool-IC-small Reactor-IC-small
Shelf 2	GRAND "DOWN" external battery pack	Pool-He1 Pool-He2 Pool-IC-large Reactor-IC-large
Shelf 3	Computer for GRAND "Up" Bernoulli disk drive Smart UPS	Pool-FC1 Pool-FC2 Pool-IC-small Reactor-IC-small Pool-He2 (signal only)
Shelf 4	Computer for GRAND "DOWN" Bernoulli disk drive Smart UPS	Pool-He1 Pool-He2 Pool-IC-large Reactor-IC-large Pool-FC2 (signal only)
Cabinet Floor	Power transformers	

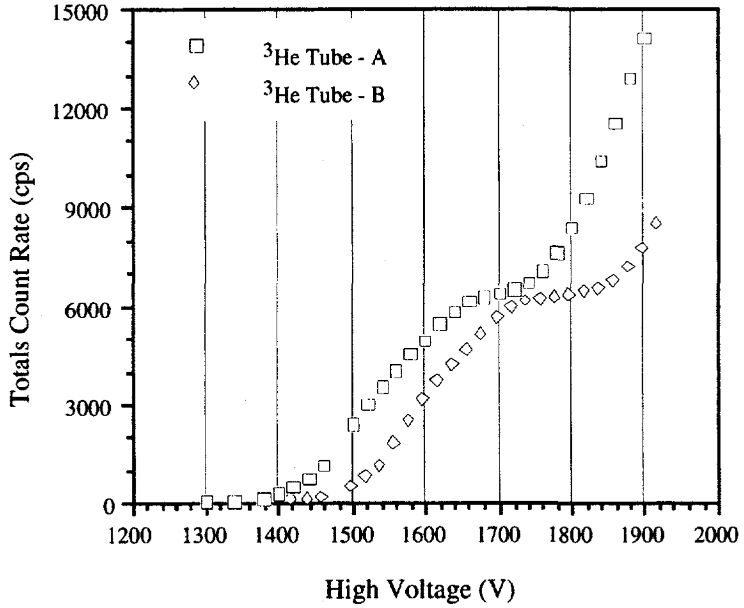

Fig. 7. The ^{3}He counting rate as a function of detector bias. The ^{3}He-A has more gain in the PDT-110A amplifier than ^{3}He-B to provide different gamma sensitivity. Both detectors were operated at 1720 V.

^{3}He-TUBE HIGH-VOLTAGE PLATEAU (cont.)

the neutron discrimination threshold at ~5 R/h and tube B, with the lower gain, will pick up gamma interference at ~50 R/h.

For the current application of the ^{3}He tubes, we are using the detectors to count neutrons from the fresh MOX fuel assemblies and gamma rays from the spent-fuel assemblies. The fresh UO_2 and MOX fuel assemblies will have less than 0.1 R/h dose levels and the spent fuel will have levels greater than 10^4 R/h. Thus, the ^{3}He tubes will only count neutrons for fresh fuel and gamma rays (saturation) for irradiated fuel. The gamma rays are primarily counted with the four ion chambers, and the ^{3}He tubes provide backup.

ION CHAMBERS

Two of the ICs are LND Model 52110; they are 16 mm in diameter with an 85.9-mm active length and are contained in a sealed stainless steel tube with a 25-mm outside diameter and a length of 187 mm. The sensitivity of the IC is 3.4×10^{-10} A/R/hr.

The other two ICs are LND Model 50346; they are 50.8 mm in diameter with a 321.1-mm active length and are contained in a sealed stainless steel tube with a 57-mm outside diameter and 373-mm length. The sensitivity of the IC is 3.5×10^{-9} A/R/hr.

The IC has a useful gain range of about eight decades when using the automatic gain-range feature. The actual background level is ~0.006 gamma units so the wings of the response peak are lost using the manual setting that spans only five decades. For the FUGM spent fuel transfer, the IC signal was ~9999 gamma units for the small IC and ~99 995 gamma units for the larger IC.

There is a relay in each detector assembly that provides for the disconnection of the ionization chamber from the signal cable. This relay allows offsets to be taken. One of the unique features of the GRAND electronics is its ability to adjust for offset currents due to moisture in connectors, damaged cables, and electronic offsets. It also serves as a useful diagnostic tool in the event of anomalous readings. This relay is a high-reliability relay and the normally closed contacts are used to disconnect the ionization chamber.

ION CHAMBERS
(cont.)

Hence, it is expected that a failure (a very unlikely event, which has never been experienced in any of the systems) would result in the loss of diagnostic capability and not in the loss of signal transmission to the GRAND.

CABLE CONNECTIONS

For the neutron detectors, the high voltage, signal, and +12 V sources are connected to the GRANDs using RG-174 coaxial cables with LEMO connectors. The ion chambers use LEMO connectors on RG-174 coaxial cable for the signal and Belden 87723 twisted paired cable for the high voltage. The large detector package has 12 cable connections (see Fig. 8) and the small detector package has 4 cable connections (see Fig. 9). Table IV gives the LEMO connector type and number for each detector package.

The two detector assemblies are each connected to redundant GRANDs indicated in Fig. 6.

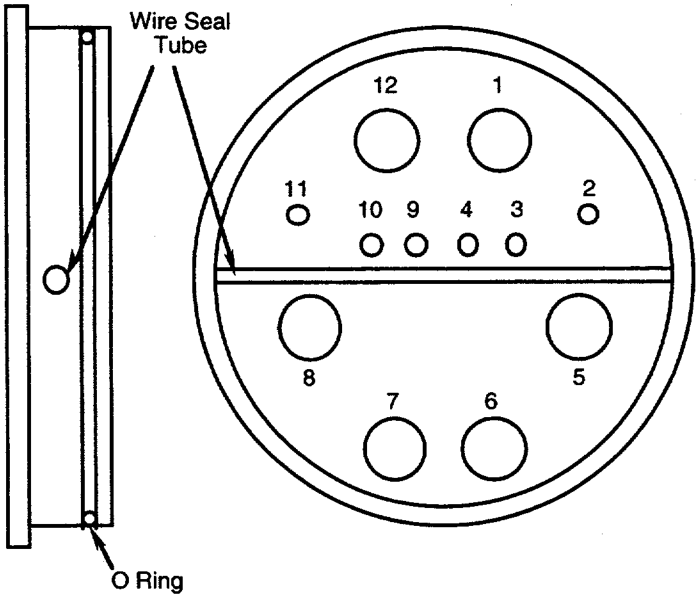

1 - He-3 Bias
2 - He-3 +12V
3 - He-3 Sig. A
4 - He-3 Sig. B
5 - Large IC Bias
6 - Large IC Signal
7 - Small IC Signal
8 - Small IC Bias
9 - FC Sig. B
10 - FC Sig. A
11 - FC +12V
12 - FC Bias

Fig. 8. Side and end-view of the connector endcap located underneath the security cover on the large detector package. The layout of the cable connectors and their function are shown.

CABLE CONNECTIONS
(cont.)

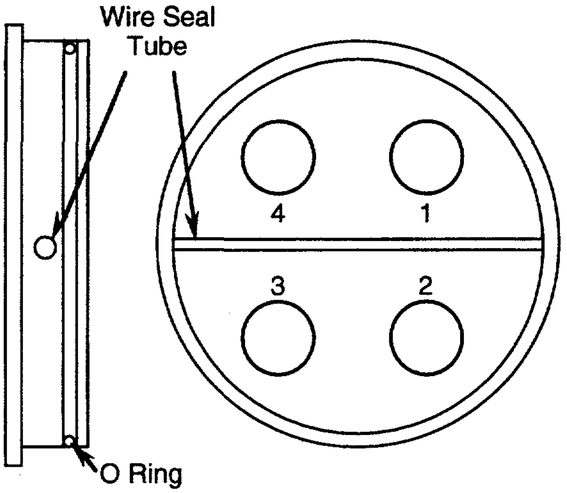

1 - Small IC Bias
2 - Small IC Signal
3 - Large IC Signal
4 - Large IC Bias

Fig. 9. Side and end-view of the connector endcap located underneath the security cover on the small detector package. The layout of the cable connectors and their function are shown.

TABLE IV. LEMO Cable Connector Types for Sockets on the Bulkhead of each Detector Package

Detector Package	Type	Number	Size	Function
Large	FFA.00.250.CLAC	6	small	He, FC-Signal; + 12 V
	FFA.0E.250.CLAC	4	large	He, FC-Bias; IC sig.
	FFA.1S.304.CLAC	2	large	IC Bias
Small	FFA.1S.304.CLAC	2	large	IC Bias
	FFA.0E.250.CLAC	2	large	IC-sig.

Two cable bundles, each consisting of five RG-174 cables and one Belden 87723 cable, connect the large detector package to the electronics cabinet. One bundle is for the ^{3}He tubes and large IC (connectors 1-6 in Fig. 8) and the other for the FCs and the small IC (connectors 7-12 in Fig. 8). One cable bundle containing two RG-174 cables and two Belden 87723 cables is used for the small detector package. Figure 9 shows the layout of the LEMO sockets in the small detector bulkhead underneath the security cover.

CABLE CONNECTIONS (cont.)

The GRANDs are labeled GRANDUP and GRANDDN. The general wiring scheme is shown in the FUGM reactor-wiring block diagram (see Fig. 6).

The cables are connected to their respective GRANDs via a ground isolation box (GIB). The purpose of this box is to provide a high AC-impedance in the ground connections between the GRANDs and the remote detector packages. This technique is to provide a degree of hardness against induced interference in the long signal cables. The signal connections are passed directly through the ground isolation box, but the ground plane on the detector side of the GIB is separated from the GRAND side ground plane with a 1-mHy inductor.

LABELS

The labels on the cables that connect to the detector package, shown in the first column of Table V, have either the word GDA (GRAND-A) or GDB (GRAND-B) as the first part of their designations. This identifies the GRAND unit to which the cable is connected. The second part of the designation indicates the GRAND connector to which the opposite end of the wire is attached.

Similarly, the labels on the cables in the electronics cabinet, second column of Table V, have the designator UP (GRAND-B) or DN (GRAND-A) indicating the GRAND unit to which the cable is connected. The second part of the designator indicates the connector the cable should be attached to on the GRAND boards.

GRAND-3 CONNECTIONS

Figure 10 shows a diagram of the edge view of the GRAND triple neutron counter (TNC) board, the ion chamber personality board, and the connectors found on them. Table V lists the labels on the cables that attach to the detector assemblies and the GRANDs along with the GRAND unit, the board to which it attaches, the type of connector on the board, and the sensor label that appears in the software. The coaxial (RG-174) and twisted pair (Belden) cables that connect the sensors to the GRANDs are approximately 70 m long.

AMPLIFIERS

The two ^{3}He tubes and two FCs have their PDT-110A amplifiers inside the sealed detector pipe. The pipe contains ~2 L of desiccant. The cables between the tubes and the PDT-110A are 20-30 cm long. The gain in the PDT amplifiers for the fission chambers was preset prior to

AMPLIFIERS
(cont.)

TABLE V. Cable Connections and Labels

70 m Cable Labels at					
Detector Assembly	Electronics Cabinet	GRAND Unit	GRAND Board	GRAND Connector	Software Label
GDB DSA-FC	UP FC-A	UP	TNC	A	Pool FC-1 (G-UP)
GDB DSB-FC	UP FC-B	UP	TNC	B	Pool FC-2 (G-UP)
N/A	DN He-B*	UP	TNC	C	Pool He-2 (G-UP)
GDB FC-Bias	UP FC Bias	UP	TNC	HV	—
GDB FC+12 V	UP FC + 12 V	UP	Side Panel	D9 (9-pin)	—
GDB IC1	UP IC1	UP	IC	SIG-1	Pool IC Small (G-UP)
GDB IC2	UP IC2	UP	IC	SIG-2	Reactor IC Small (G-UP)
GDB IC1 Bias	UP IC Bias	UP	IC	Bias	—
GDB IC2 Bias	(none)**	UP	IC	Bias	—
GDA DSA He-3	DN He-A	DN	TNC	A	Pool He-1 (G-DN)
GDA DSB He-3	DN He-B	DN	TNC	B	Pool He-2 (G-DN)
N/A	UP FC-B*	DN	TNC	C	Pool FC-2 (G-DN)
GDA He-3 Bias	DN He-Bias	DN	TNC	HV	—
GDA + 12V	DN He + 12 V	DN	Side Panel	D9 (9-pin)	—
GDA IC1	DN IC1	DN	IC	SIG-1	Pool IC Large (G-DN)
GDA IC2	DN IC2	DN	IC	SIG-2	Reactor IC Large (G-DN)
GDA IC1 Bias	DN IC-Bias	DN	IC	Bias	—
GDA IC2 Bias	(none)**	DN	IC	Bias	—

*Cross wired in cabinet for redundancy
**Split occurs at Isolation Box

Triple Neutron Counter (TNC) Board

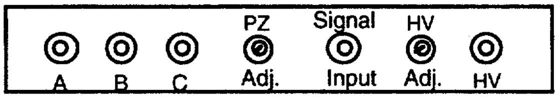

Ion Chamber (IC) Board

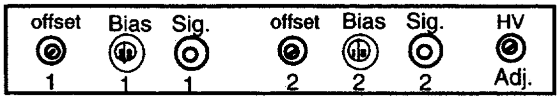

Fig. 10. Edge view of the LEMO connector locations on the Triple Neutron Counter Board and the Ion Chamber Board installed in the GRAND.

AMPLIFIERS
(cont.)

installation using the same criteria as for the Fork Detector.[2] This corresponds to a count rate less than 0.5 counts/s when a neutron source is not present. This signal is generated by the alpha particles emitted from the uranium lining in the fission chamber. The ^{3}He detector bias in the GRAND was adjusted at the time of calibration to provide the desired sensitivity level. The hv was set at 1720 V.

PERFORMANCE CHARACTERISTICS

Prior to installation, the performance of the ^{3}He tubes and the ICs was measured at Los Alamos using an ^{241}Am gamma-ray source and a ^{252}Cf neutron source. The cable between the detector package and the GRAND was 70 m long to check for possible attenuation of the signals.

^{3}He TESTS

To measure the efficiency of the ^{3}He neutron detectors for source neutrons at different distances from the detector pipe, we counted a ^{252}Cf source (CR-11) as a function of separation distance. Figure 11 shows the counting rate in the two ^{3}He detectors measured at Los Alamos before the system was shipped. As the neutron source moves away from the detector, the room-scattered neutrons contribute an increasing fraction to the total counts. To simulate the scattering conditions at the Fugen Reactor, we positioned the detector pipe adjacent to a thick (~1 m) concrete wall with the detector package about 0.8 m above the concrete floor.

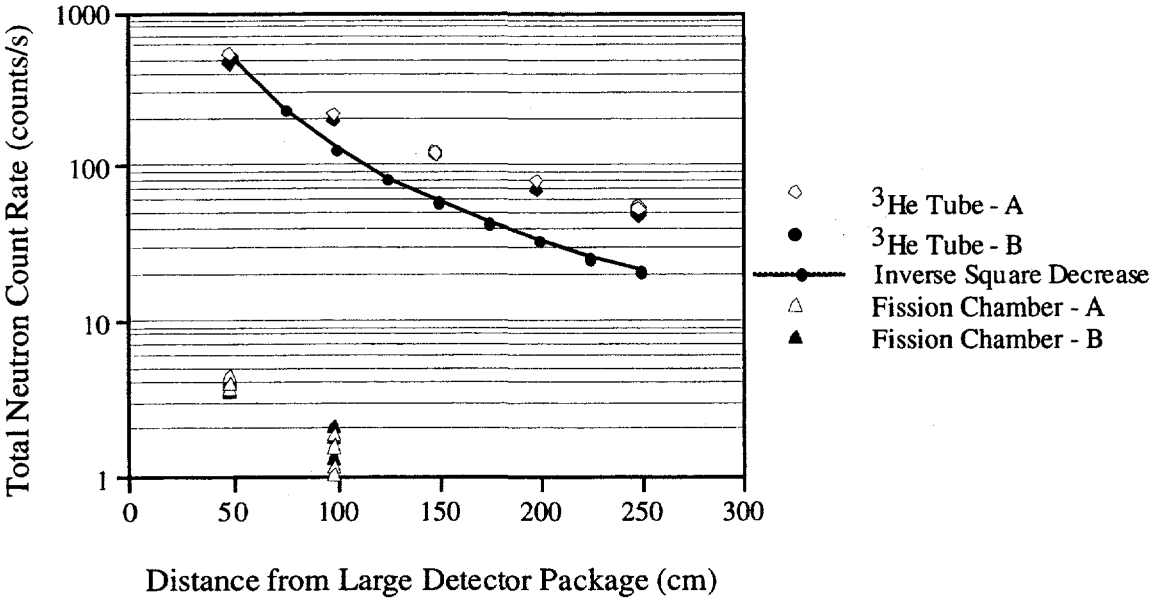

Fig. 11. ^{3}He and fission chamber detector response per source neutron as a function of distance to the ^{252}Cf neutron calibration source.

^{3}He CALIBRATION (cont.)

In the absence of scattered neutrons, we would expect the counting rate to decrease as the inverse square of the distance. Figure 11 shows the inverse square decrease that is normalized to the first data point at 50 cm. The distance from the detector package to the closest position of the fuel assembly is ~0.6 m, so the ^{3}He counting efficiency is ~0.5%.

The two detector assemblies that are separated by ~2 m in the reactor annulus (see Fig. 5) provide data on the direction of motion and speed of the spent-fuel-rod transfers. The fuel chute in the reactor annulus has a large diameter (~1 m) and a considerable amount of radiation streams through the chute before the fuel assembly enters the annulus. Thus, the wings of the fuel transfer event are not used to establish the speed or the direction of motion and we use the maximum signal levels from detectors A and B to determine the transit time and the direction of motion. The 1-m-diameter transfer chute has a coaxial inner pipe ~50 cm in diameter that is filled with water during the fuel transfer. Thus, both the neutron and gamma-ray signals are attenuated by roughly two orders of magnitude by the water (~20 cm thick) and steel (~1-cm thick) walls.

IC TESTS

For measuring the relative gamma-ray dose, the ICs have a very wide dynamic range over which the IC response is proportional to the gamma source strength whereas the response of the ^{3}He tubes is nonlinear and begins to saturate at dose levels of approximately 5-10 R/h. In each detector assembly there are two ICs of different sensitivities. This further extends the dynamic range of the fuel-flow monitoring system and provides redundant data on the direction of motion and speed of the fuel rod transfers.

CALIBRATION PROCESS

At the time of installation, the ICs, FCs, and ^{3}He tubes were calibrated using fuel transfers through the transfer chute. The transfer takes the rods from the reactor location past the FUGM detector packages to the storage pool (OUT) area during the unloading phase and the reverse direction during the reload phase (IN). Table VI summarizes the fuel movements used during the calibration.

For test purposes, fuel assemblies were moved forward and backward through the chute to evaluate the capability of the detector system to measure the direction of motion.

TABLE VI. Summary of Fuel Transfers Performed During Calibration Exercise

No.	Date	Time	Fuel Type	Transfer Direction	Burnup (MWD/T)
10	Nov. 13, 1995	11:05-11:23	Fresh MOX	IN	—
11	Nov. 13, 1995	11:23-11:50	Fresh MOX	OUT	—
12	Nov. 13, 1995	12:30-13:05	Cover plug	IN	—
13	Nov. 13, 1995	13:05-13:25	Cover plug	OUT	—
14	Nov. 13, 1995	13:27-13:49	Cover plug	IN	—
52	Nov. 14, 1995	18:24-18:48	Irradiated UOX	IN	14 000
56	Nov. 14, 1995	22:33-22:55	Irradiated MOX	IN	12 000
60	Nov. 15, 1995	02:14-02:35	Irradiated MOX	IN	12 000
63	Nov. 15, 1995	4:29-4:50	Transfer container	OUT	—
64	Nov. 15, 1995	5:11-5:32	Irradiated MOX	IN	12 000
65	Nov. 15, 1995	5:40-6:01	Transfer container	OUT	—
66	Nov. 15, 1995	6:35-7:00	Cover plug	IN	—
67	Nov. 15, 1995	7:11-7:32	Transfer container	OUT	—
68	Nov. 15, 1995	7:47-8:07	Irradiated UOX	IN	14 000
69	Nov. 15, 1995	8:42-9:49	Transfer container	OUT	—
70	Nov. 15, 1995	10:09-10:30	Cover plug	IN	—
71	Nov. 15, 1995	10:40-11:04	Transfer container	OUT	—
72	Nov. 15, 1995	11:24-11:45	Irradiated MOX	IN	12 000
76	Nov. 15, 1995	15:05-15:26	Irradiated UOX	IN	24 000
80	Nov. 15, 1995	15:05-15:26	Irradiated UOX	IN	24 000
84	Nov. 15, 1995	21:39-22:00	Fresh UOX	IN	—
88	Nov. 16, 1995	0:51-1:14	Fresh UOX	IN	—
92	Nov. 16, 1995	5:10-5:33	Fresh MOX	IN	—

CALIBRATION PROCESS (cont.)

The data were collected with a 10-s time frequency and the transfer time offset was ~30 s between the reactor-side detectors and the pond-side detectors.

The direction of motion also can be detected by the shape of the neutron and gamma peaks. The data collection software has a filter that compresses the data by a factor of 50 when the counting rates in all sensors are not changing for a preset period of time. To come out of the filter mode, two adjacent data points must deviate from the average by more than 3σ. These statistical criteria can be changed in the parameter file.

DATA ANALYSIS

Four varieties of fuel assemblies are available for transfer in addition to several special varieties as indicated below.

Fresh MOX
Fresh UO_2
Irradiated MOX
Irradiated UO_2
Irradiated special fuel
Special seal and cover plugs

The FUGM detector packages were designed to measure the fuel transfer parameters listed in Table VII.

Table VIII lists the different types of fuel assemblies and the responses from the radiation sensors in the FUGM detector packages. The multiple sensors were selected to cover the wide radiation levels from the fresh and irradiated fuel assemblies. The neutron and gamma emission levels change by about seven orders of magnitude between the fresh and irradiated fuel assemblies. The ^{3}He tubes are used to measure the neutrons from the fresh MOX and the FCs are used to measure neutrons from irradiated fuel in the high gamma-ray backgrounds. The large ICs measure the low-level gamma-ray emission assemblies and the small ICs measure the gamma emission from the irradiated fuel. In Table VIII, the designation “P” corresponds to a primary radiation sensor for fuel type identification, the designation “s” corresponds to a secondary sensor (at the edge of detectability), and “sat.” corresponds to a saturation signal that gives redundancy for the irradiated fuel transfer. The neutron/gamma ratio is used to give additional identification for some of the fuel types.

DATA ANALYSIS
(cont.)

TABLE VII. Fuel Transfer Parameters Measured with FUGM

Parameters Determined	Attributes Measured
1. Number of transfers	Gross gamma and gross neutron counts
2. Time of transfer	Time and date of maximum count rate
3. Direction of transfer	Radiation time pattern and time interval between detectors A & B
4. Speed of fuel transfer	Time interval between detectors A & B
5. Size of fuel assembly	Radiation time pattern
6. Relative burnup	Neutron count rate
7. Type of fuel assembly	Neutron rate, gamma rate, and neutron/gamma ratio

TABLE VIII. Fugen Sensor Array Response for Each Fuel Type Measured

Fuel Type	Fission Chamber	He-3 Tube	Large IC	Small IC	n/g Ratio
Fresh MOX	s	P	o	o	P
Fresh UOX	o	o	o	o	o
Irrad. MOX	P	P (sat.)	P	P	P
Irrad. UOX	P	P (sat.)	P	P	P
Irrad. Plug	o	P (sat.)	P	P	P

P = Major Sig., s = Minor Sig., sat. = Saturation, and o = no information

The determination of the fuel type is a more complex question than the number and direction of fuel transfers. The calibration provides a signal range for each of the sensors corresponding to the different fuel types listed in Table VIII.

The fuel type is identified by comparing the measured neutron and gamma signal rates and ratios with a matrix of the type shown in Table IX. The absolute magnitude of the count rates observed in each detector for all the fuel types is summarized in this table. The units for the neutron detectors are counts per second and the values for the gamma detectors are expressed as relative gamma units (RGUs). The RGUs are proportional to the current pulses produced from the ICs. Initially, the data evaluation will be done manually but

DATA ANALYSIS
(cont.)

software is under development at Los Alamos National Laboratory under the Program of Technical Assistance for IAEA Safeguards (POTAS) to automate this activity.

The values in Table IX are averages with standard deviations for several measurements of similar fuel types. The data from which these values were calculated are listed in Table X. A correction for background was not made for this data. Each value in Table X corresponds to an integral average of portions of the fuel transfer pattern measured from a given detector. Figure 12 shows a representative fuel transfer pattern obtained from a gamma-ray detector (Fig. 12a) and a neutron detector (Fig. 12b). When the ^{3}He detectors are measuring spent fuel, the fuel transfer pattern will look more like Fig. 12a because of the gamma-ray pileup.

The highlighted regions in Fig. 12 show the areas that are integrated to obtain the values in Table X. For both the gamma-ray and the neutron detectors, the three channels surrounding the peak, the centroid plus 1 point on each side of the centroid, are used. The neutron detectors have a second component that consists of the 50 channels preceding or following the peak area depending upon whether the fuel assembly is entering (Fig. 12) or leaving the reactor refueling pond. The calculation of the average peak areas is summarized below:

Gamma

$$A_\gamma = \frac{[P_{i-1} + P_i + P_{i+1}]}{3}$$

Neutron, fuel assembly entering

$$A_n = \left[\{P_{i-1} + P_i + P_{i+1} \} + \sum_{j=i-2}^{i-51} Cj \right] \frac{1}{53}$$

Neutron, fuel assembly leaving

$$A_n = \left[\{P_{i-1} + P_i + P_{i+1} \} + \sum_{j=i+2}^{i+51} Cj \right] \frac{1}{53}$$

where p_i is the count rate at the peak centroid
Cj is the count rate in the continuum before (IN) or after (OUT) the peak.

DATA ANALYSIS (cont.)

TABLE IX. FUGM Calibration Data Range

	Pool						Reactor Side	
Fuel Type	FC1	FC2	He1	He2	Lg IC A	Sm IC A	Lg IC B	Sm IC B
Fresh MOX	0.11 ± 0.04	1.1 ± 1.4	17.2 ± 0.3	13.6 ± 1.2	o	o	o	o
Fresh UOX	o	o	o	o	0.255*	o	0.073*	o
Irrad. MOX	10.6 ± 0.2	24.2 ± 1.9	2.83e4 ± 0.06e4	8.75e4 ± 0.08e4	3.42e4 ± 0.09e4	2130 ± 107	2.38e4 ± 0.08e4	2340 ± 187
Irrad. UOX (14)	0.55 ± 0.02	1.7 ± 0.4	2.68e4 ± 0.15e4	8.55e4 ± 0.21e4	3.26e4 ± 0.1e4	2090 ± 28	2.02e4 ± 0.08e4	2090 ± 316
Irrad. UOX (24)	1.19 ± 0.02	3.8 ± 0.5	2.85e4	8.94e4	3.57e4 ± 0.03e4	2330 ± 16	2.45e4 ± 0.03e4	2570 ± 26
Irrad. Plug	o	o	0.20 ± 0.06	5.5 ± 1.7	129 ± 26	3.0 ± 0.5	55 ± 10	2.7 ± 0.7

*The measured gamma radiation is from the transfer basket rather than the UO_2.

DATA ANALYSIS
(cont.)

TABLE X. Integral Signal Averages for Individual Fuel Assembly Transfers.

	Fresh MOX				Fresh UOX		Irradiated MOX (12 GWD/t)			
No.	10	24	40	92	84	88	56	60	64	72
FC 1	0.2	0.1	0.1	0.1	o	o	11	10	10	10
FC 2	0.38	0.36	0.38	3.3	o	o	24	22	24	27
He 1	18	17	17	17	o	o	2.91e4	2.79e4	2.85e4	2.79e4
He 2	13	13	13	15	o	o	8.83e4	8.56e4	8.81e4	8.70e4
Lg IC A	o	o	o	o	0.26*	0.25*	3.74e4	3.43e4	3.50e4	3.30e4
Sm IC A	o	o	o	o	o	o	2140	2240	2160	1990
Lg IC B	o	o	o	o	0.073*	0.073*	2.42e4	2.28e4	2.47e4	2.34e4
Sm IC B	o	o	o	o	o	o	2460	2100	2510	2300

*The gamma counts come from the contamination in the carrier tube.

TABLE X. (con't)

	Irrad.UOX (14 GWD/t)		Irrad.UOX (24 GWD/t)		Irradiated Plug			
No.	52	68	76	80	54	62	70	82
FC 1	0.57	0.53	1.2	1.2	o	o	o	o
FC 2	1.4	2.0	3.5	4.2	o	o	o	o
He 1	2.79e4	2.57e4	2.85e4	2.85e4	0.11	0.26	0.21	0.21
He 2	8.68e4	8.40e4	8.94e4	8.94e4	3.0	6.4	6.2	6.7
Lg IC A	3.33e4	3.19e4	3.60e4	3.53e4	95	157	133	131
Sm IC A	2110	2070	2320	2340	2.3	3.3	3.3	3.0
Lg IC B	1.97e4	2.08e4	2.43e4	2.47e4	40	62	59	57
Sm IC B	2310	1870	2590	2550	1.7	3.0	2.7	2.7

DATA ANALYSIS
(cont.)

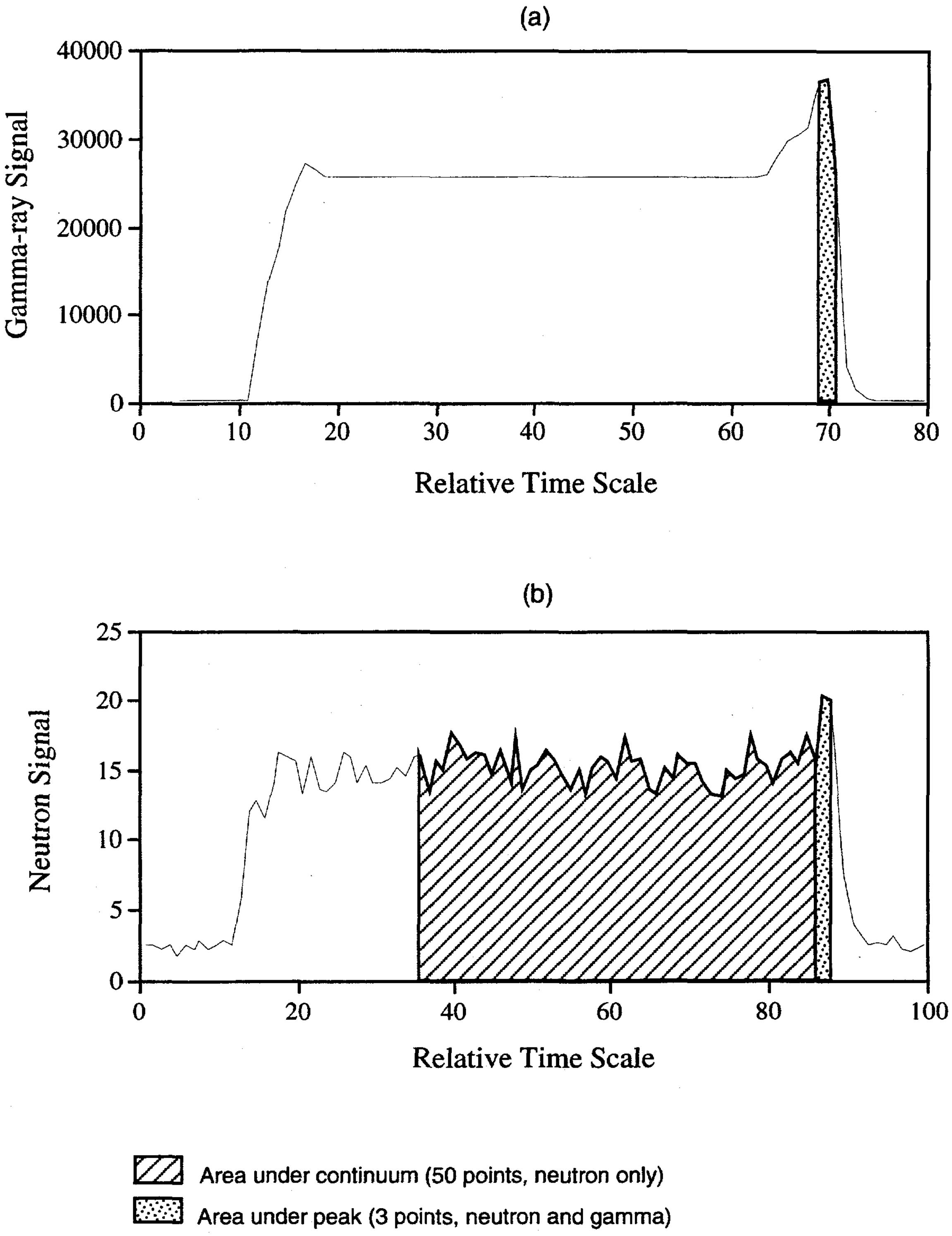

Fig. 12. Representative fuel transfer signal for gamma-ray (a) and neutron (b) detectors illustrating the regions used to calculate the average signal for each detector type.

FUEL TRANSFER PROCESS

To understand the measured radiation patterns, it is necessary to describe the procedure for the fuel transfer through the chute. Figure 13 is an overview of the fuel assembly transfer chute between the refueling pond inside the reactor containment building and the fuel transfer pool inside the spent-fuel storage pool building. Figure 14 shows a simplified diagram of the annulus between the reactor and the exterior pool with the transfer chute and a fuel transfer basket. The fuel assembly is placed in a transfer basket that is lowered through the chute using a crane. The transfer pipe (508-mm ID) is filled with water during the transfer. The fuel assembly moves at a rate of ~6 m/min to the position shown in Fig. 14. At this position, the assembly stops for ~12 min. while the upper (reactor side) handling device releases and the basket and the lower (pool side) device engages the basket. The basket then exits the transfer chute at a rate of ~6 m/min. All of the fuel assemblies, cover plugs, and cover seals move in and out of the reactor using the transfer basket and the same handling procedure.

The fuel assemblies are ~4 m long. The maximum counting rate is observed when the center (highest burnup) region of the assembly is directly adjacent to the detector. Detectors A and B (see Fig. 14) are separated by ~3 m of travel so the transit time interval is ~30 s. This time offset provides the direction of motion. The time pattern from a single detector also provides the direction of transfer for redundancy.

FUEL TRANSFER PROCESS
(cont.)

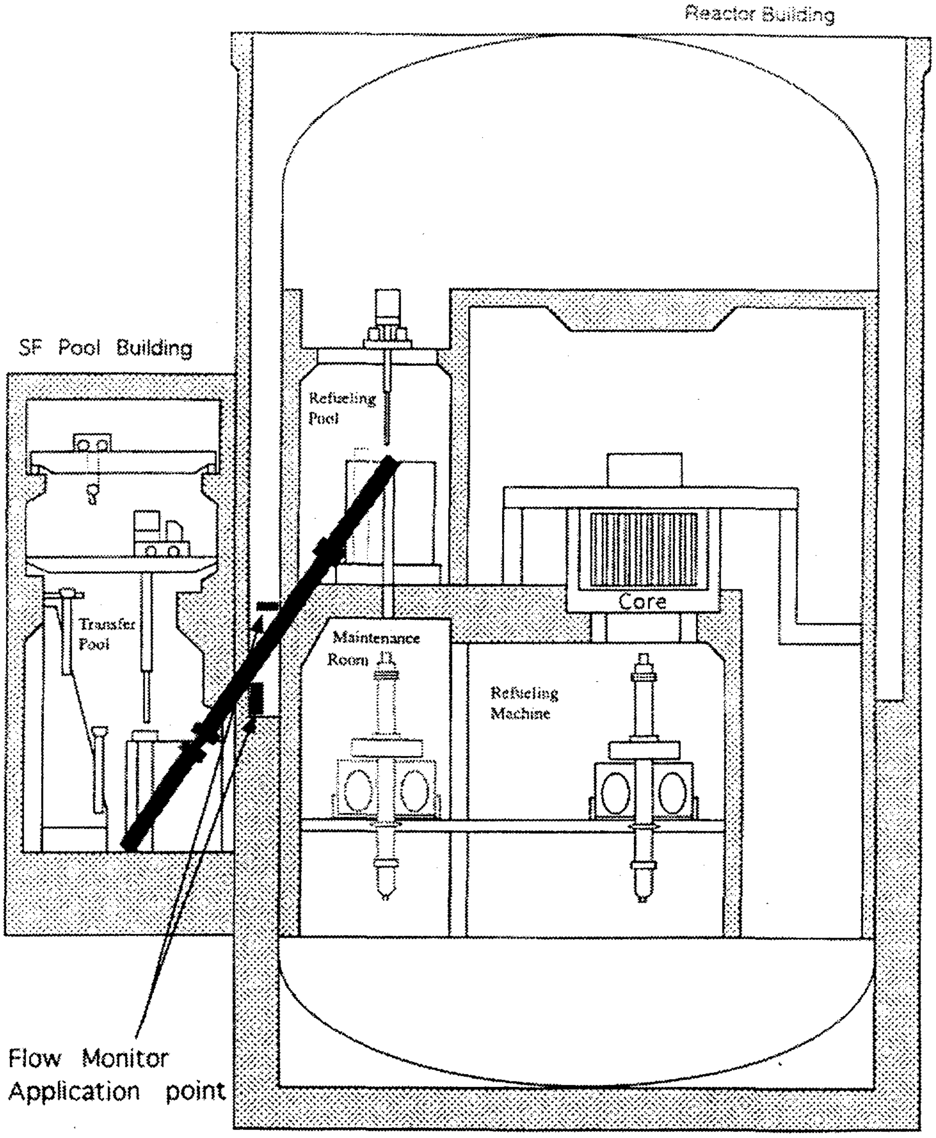

Fig. 13. Diagram of the Reactor Containment Building and the Spent Fuel Storage Building showing the location of the fuel transfer chute and the FUGM detector packages.

FUEL TRANSFER PROCESS
(cont.)

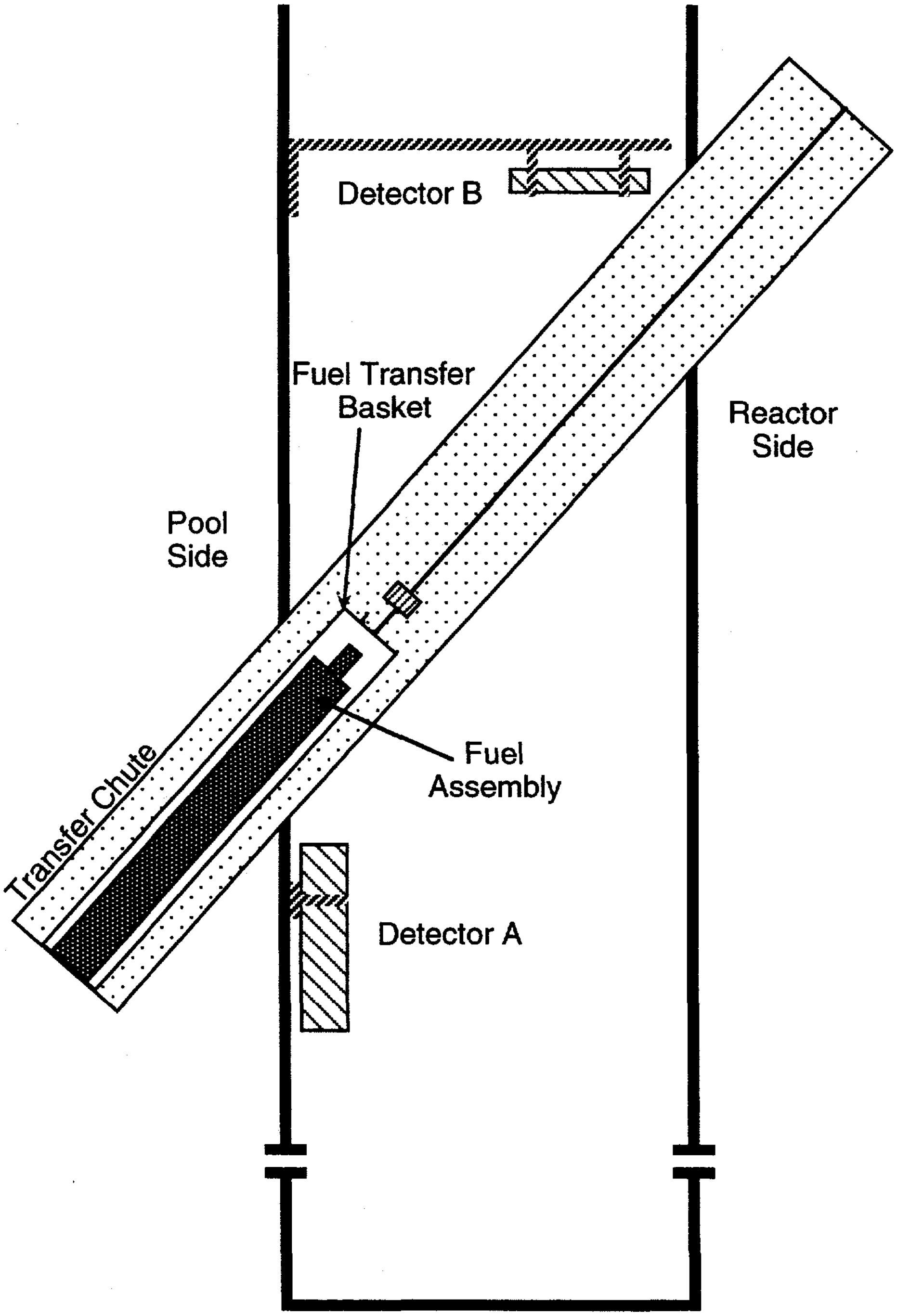

Fig. 14. Schematic diagram of the Fugen Reactor annulus showing the fuel transfer chute and the fuel assembly stopping position during the transfer.

FRESH MOX

For test and calibration at the time of installation of the FUGM system, the different types of fuel assemblies were transferred through the chute. The results for the transfer of a fresh MOX assembly are shown in Fig. 15. For the test, the assembly was transferred in both directions; first into the reactor and then back to the storage pool.

The sensors that can be used to evaluate the transfer activity are listed in Table VIII. The primary sensors for the fresh MOX transfer are the two ^{3}He detectors that measure the neutron emission from the plutonium spontaneous fission and (α,n) reactions. This neutron signal is also detected in the two fission chambers at a very low rate as shown in Table IX. The fuel assembly is inside the water-filled pipe that attenuates the neutron and gamma signals by about two orders of magnitude.

The gamma signal from the fresh MOX is very low after the attenuation by the water (~20 cm) and the steel (~2 cm) and it cannot be detected by the ICs. However, the transfer basket contains some contaminated material near its bottom and this material gives a spike in all of the ICs as the basket passes through the chute. For irradiated fuel this spike is negligible and it is buried in the primary signal, but for fresh UO_2 and fresh MOX, the gamma spike is clearly visible and it can be seen as the basket moves in both directions.

Figure 15 shows the double (in and out) transfer pattern for the fresh MOX where the top curve corresponds to ^{3}He-1, the second curve corresponds to FC-1, and the third trace corresponds to the large IC (pool side). The only IC activity is the spikes that occur as the basket passes the pool-side detector. Figure 16 shows the same double transfer where the top curve is ^{3}He-2, the second curve is the large IC (pool), and the third curve is the large IC (reactor). The direction of motion is shown by the neutron pattern as well as the time off-set in the gamma spikes.

The fresh MOX transfer is identified by the combination of a ^{3}He neutron signal in the range of 15-30 counts/s together with a negligible gamma signal except for the carrier basket spike. The low-level FC rate of ~0.3 counts/s can be used as a secondary signal of neutrons. The ^{3}He counting efficiency is typically a factor of 100 larger than the FC counting efficiency.

FRESH MOX
(cont.)

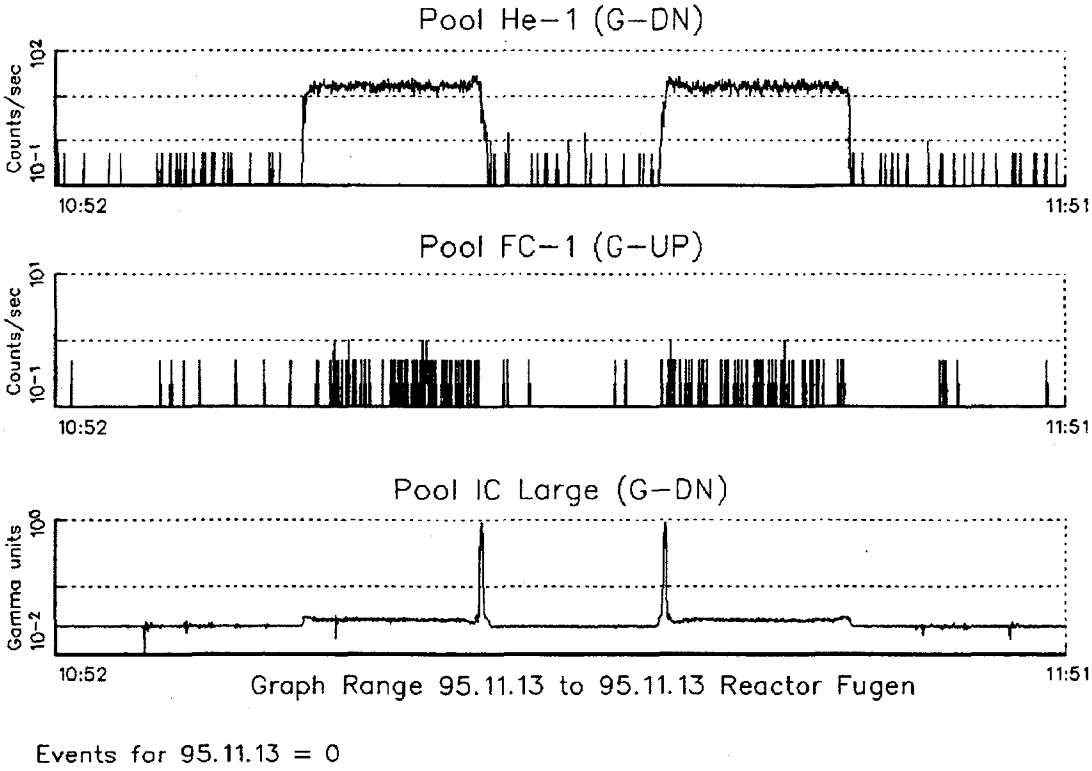

Fig. 15. Fuel transfer signal for fresh MOX assembly moving into the reactor from the transfer pool followed by a return transfer to the pool. The top curve corresponds to ^{3}*He-1 (neutrons), the middle curve corresponds to FC-1 (neutrons), and the bottom curve corresponds to the large IC (pool) [log scale].*

FRESH MOX
(cont.)

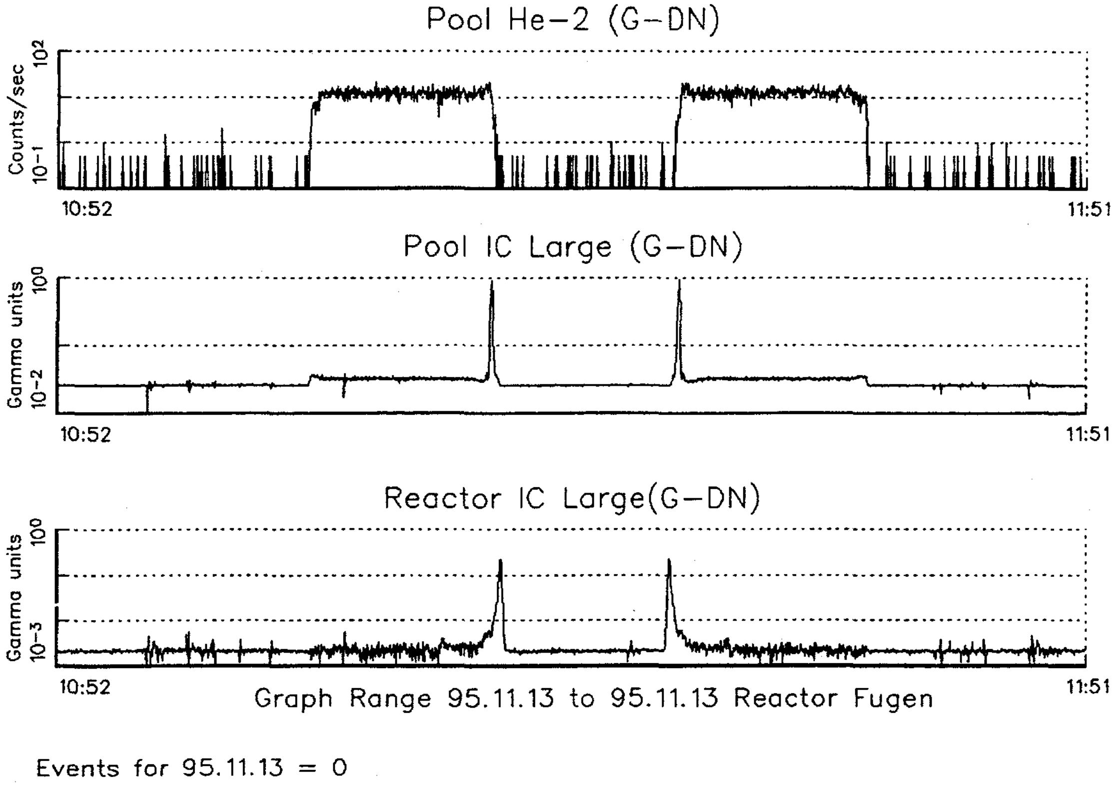

Fig. 16. Double fuel transfer (in and out) for the fresh MOX assembly where the top curve corresponds to ^{3}*He-2, the second curve is the large IC (pool), the third curve is the large IC (reactor), [log scale].*

IRRADIATED UOX

The primary signal for an irradiated UOX transfer is the gamma-ray patterns in the ICs with four-fold redundancy and the gamma-ray pileup in the ^{3}He detectors with two-fold redundancy. The two FCs provide a low-level signal (~1 count/s) for the neutron emission from the curium in the irradiated fuel.

Figure 17 shows the fuel transfer pattern for irradiated UOX moving into the reactor. The top curve corresponds to the small IC (pool), the second curve corresponds to the ^{3}He-2 detector (pool) and the bottom curve corresponds to the FC-1 (pool). Figure 18 shows the large IC (pool) and the large IC (reactor). The gamma patterns show the distinctive shape of a church with a 12-min long plateau followed by a sharp peak at one end that is ~20 s long. The plateau is caused by the fuel assembly being held in the lower position shown in Fig. 14 while the fuel transfer handling apparatus is switching from the lower (pool side) device to the upper (reactor side) device. In this position, only the top end of

IRRADIATED UOX
(cont.)

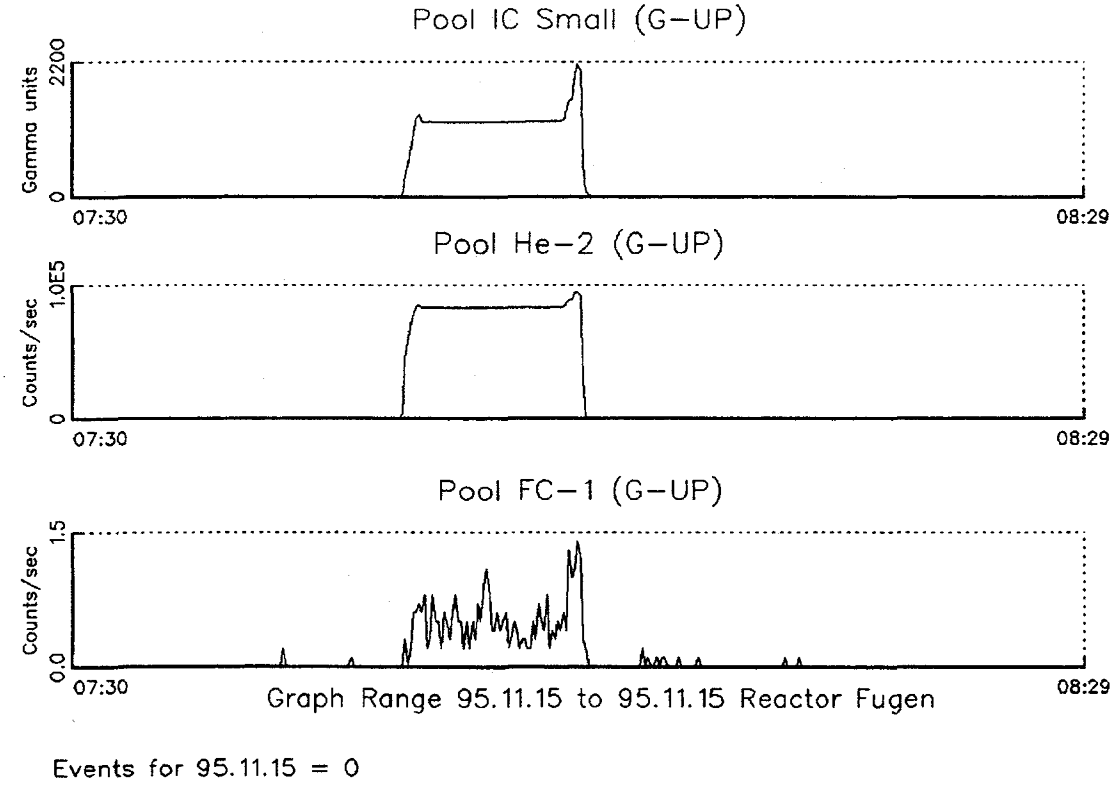

Fig. 17. Fuel transfer pattern for an irradiated UOX assembly moving from the transfer pool to the reactor. The top curve is the small IC (pool); the second and third curves are He-2 and FC-1, respectively (linear scale).

IRRADIATED UOX
(cont.)

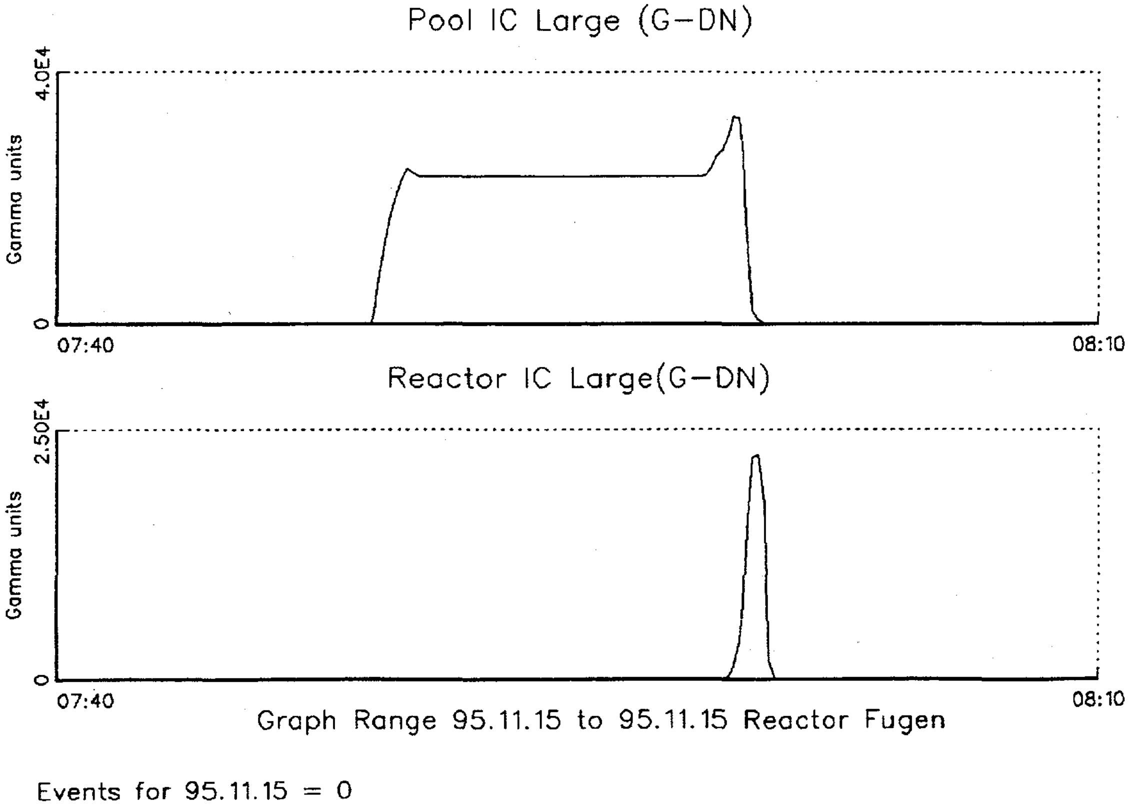

Fig. 18. Fuel assembly transfer patterns for irradiated UOX where the top curve corresponds to the large IC (pool) and the bottom curve corresponds to the large IC (reactor). The 30-s offset in the peaks gives the direction of transfer (linear scale).

the fuel assembly is exposed to the detectors. After the ~12 min hold, the fuel assembly is moved past detector A giving a strong signal peak when the center of the assembly is directly above detector A. About 30 s later, the center of the assembly passes next to detector B giving the peak in the ICs of detector B. The peak to plateau ratio of detector B is larger than for detector A because the fuel parking position is further from B than A as shown in Fig. 14.

The primary identification signature for irradiated UOX fuel is the intense gamma signals in all of the ICs, together with low counting rates in FC-1 and FC-2 to show the neutron

IRRADIATED UOX
(cont.)

emission. The direction of motion can be determined from the IC peak offsets or the signal patterns or both. There is six-fold redundancy in the gamma signals and two-fold redundancy in the neutron signals in the FCs.

IRRADIATED MOX

The transfer of irradiated MOX fuel gives signals and patterns that are similar to the irradiated UOX. However, the irradiated MOX has a neutron signal level that is about an order of magnitude larger than the signal level from the irradiated UOX of similar burnup.

Figure 19 shows the transfer of an irradiated MOX fuel assembly (12 000 MWd/tU) from the pool to the reactor. The top curve corresponds to the large IC (pool), the second curve corresponds to the FC-1, and the third curve corresponds to the FC-2. FC-2 shows a higher signal rate and background rate than FC-1 because the preamplifier has a higher gain in FC-2 compared to FC-1. Figure 20 shows the same transfer where the top curve is the large IC (pool), the second curve is the large IC (reactor), and the bottom curve is the small IC by the reactor. The curves have the same general shape as the UOX and the direction of motion can be determined by the pattern shape and/or the time offsets in peaks for the ICs in detectors A and B. The neutron rates and the neutron gamma ratios are used to distinguish irradiated UOX from irradiated MOX.

For irradiated fuel, the ^{3}He signal represents gamma pileup rather than neutron counts. Figure 21 shows a comparison of the large IC (pool) with the ^{3}He-1 (pool). We see that the ^{3}He pattern is similar to the IC pattern.

IRRADIATED MOX
(cont.)

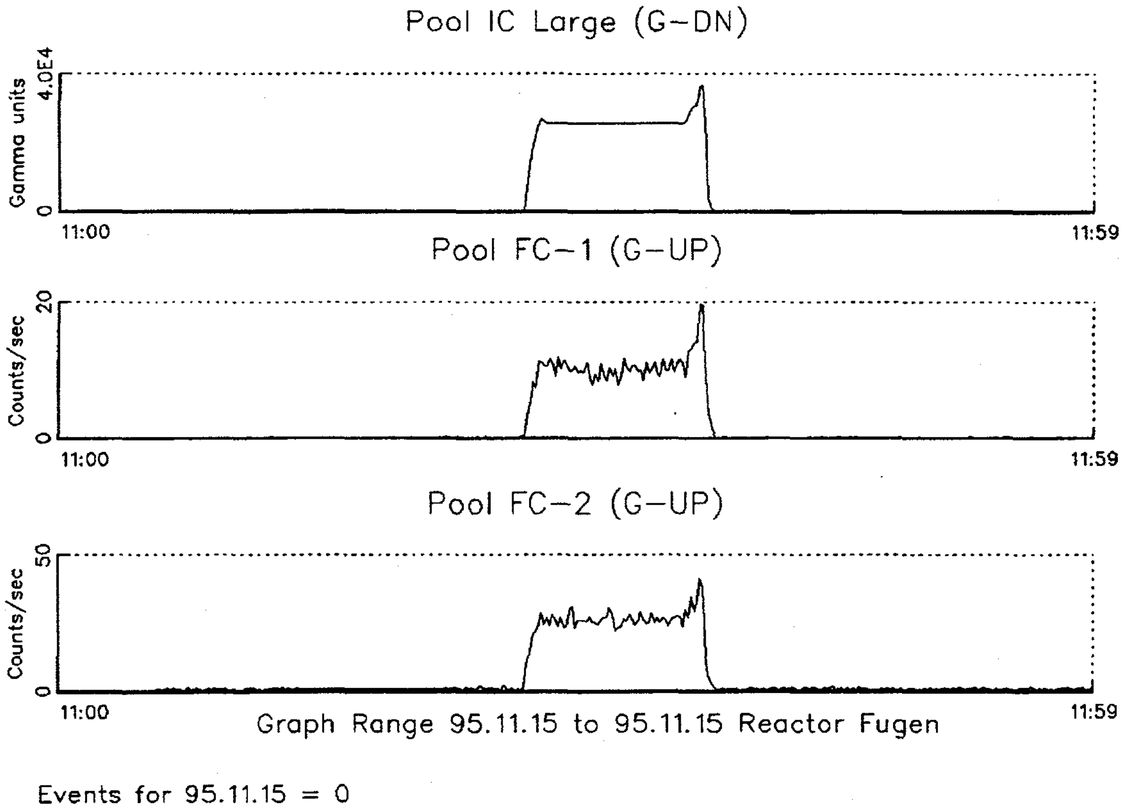

Fig. 19. Fuel assembly transfer pattern for an irradiated MOX assembly where the top curve corresponds to the large IC (pool), the middle curve corresponds to FC-1 (neutrons), and the bottom curve corresponds to FC-2 (neutrons) (linear scale).

IRRADIATED MOX
(cont.)

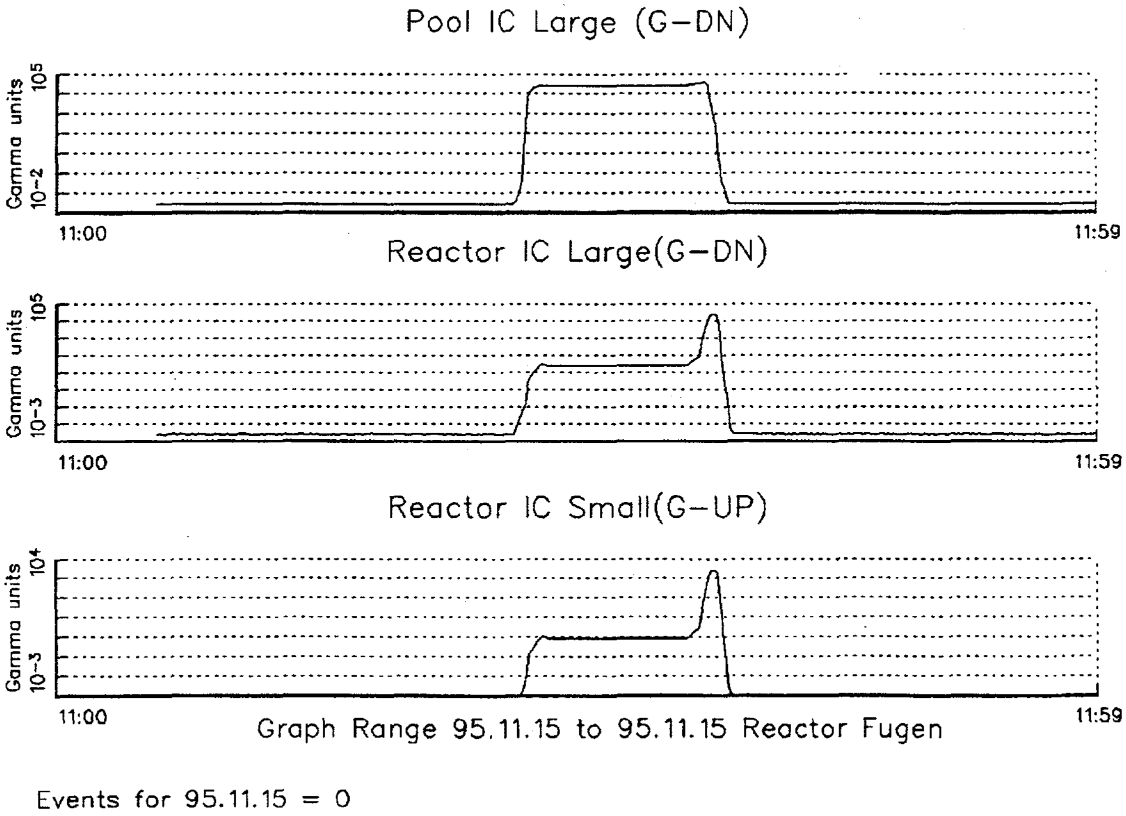

Fig. 20. Fuel assembly transfer pattern for irradiated MOX where the top curve corresponds to the large IC (pool), the second curve corresponds to the large IC (reactor), and the bottom curve corresponds to the small IC (reactor) (log scale).

IRRADIATED MOX
(cont.)

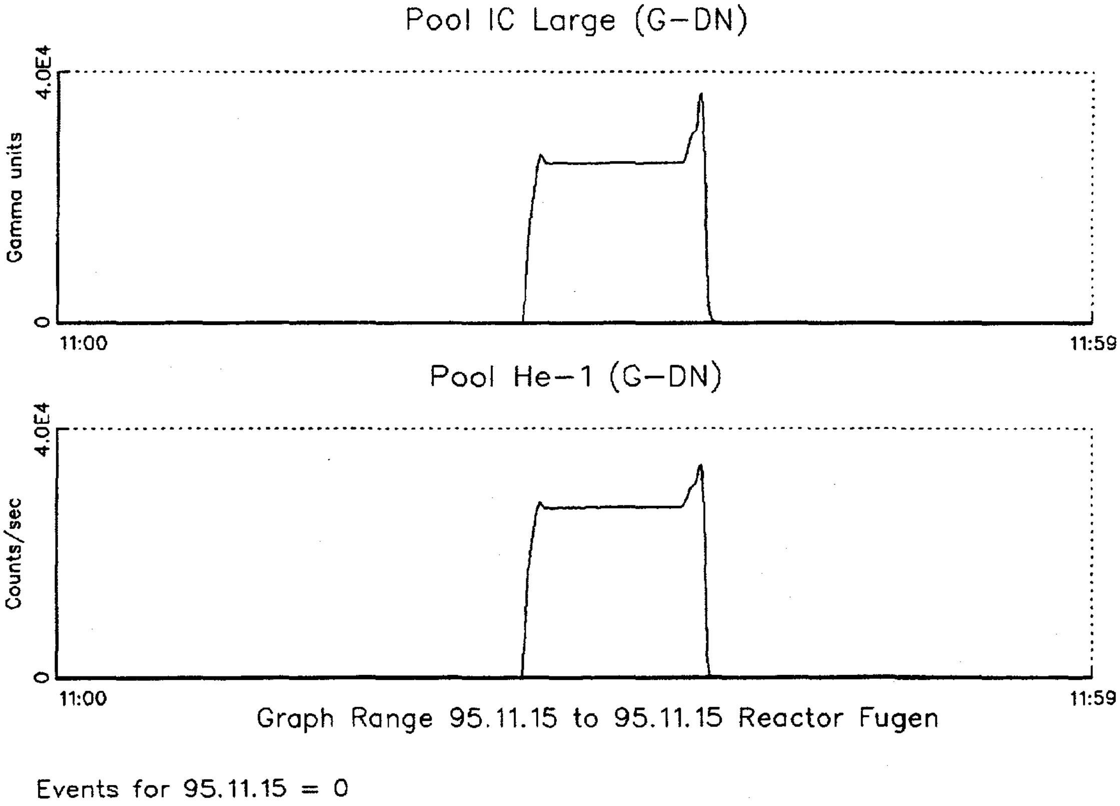

Fig. 21. Fuel assembly transfer pattern for irradiated MOX where the top curve corresponds to the large IC (pool) and the bottom curve corresponds to the ^{3}He-1 gamma-ray pileup (linear scale).

IRRADIATED REACTOR COMPONENTS

Irradiated components other than reactor fuel assemblies are passed through the transfer chute. Each fuel assembly has a reactor cover plug that is transferred in and out of the reactor at the time of fuel shuffling. The reactor cover plugs are about the same length as fuel assemblies; however, only one end is irradiated. The fuel transfer basket is used to transfer the cover plugs and the shorter fuel cover seals.

For calibration test purposes, a fuel cover plug was transferred into the reactor followed by a return out of the reactor to the transfer pool. Figure 22 shows the cover plug transfer into and out of the reactor. The top curve corresponds to the large IC (pool) signal, the second curve corresponds to the FC-1 (background level), and the bottom

IRRADIATED REACTOR COMPONENTS
(cont.)

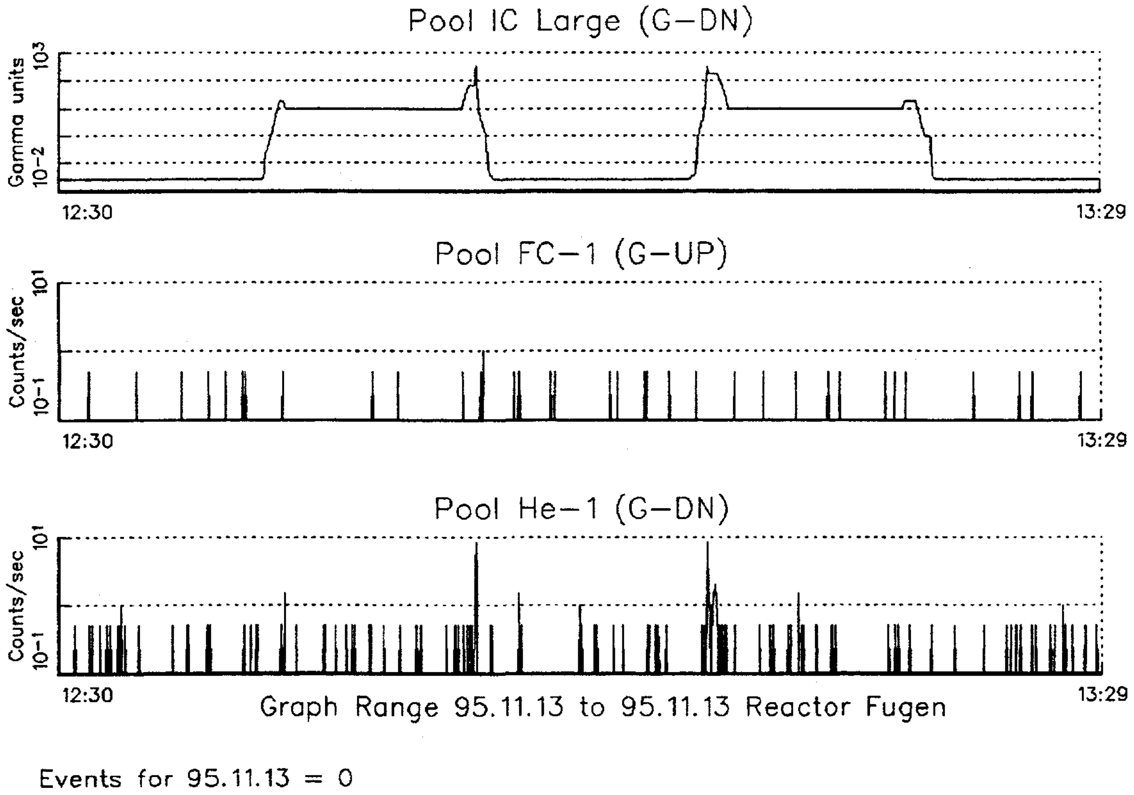

Fig. 22. Double cover-plug transfer into and out of the reactor where the first curve corresponds to the large IC (pool), the middle curve is the FC-1, and the bottom curve is ^{3}He-1 (log scale).

curve corresponds to the ^{3}He-1 (background). There is a small gamma pileup peak in the ^{3}He-1 signal as the hot portion of the cover plug passes over detector A. Figure 23 shows the pattern for a double cover-plug transfer for the small IC (pool) and the small IC (reactor). The high peak-to-plateau ratio in the small IC (reactor) is a result of the short length of the irradiated zone and its position far from detectors A and B during the 12-min stop position.

The primary signal for the cover-plug transfer is the large IC (pool) and the absence of neutron counts in the FC and ^{3}He (plateau region). The IC signal level for the cover-plug transfer is roughly three orders of magnitude lower than the

IRRADIATED REACTOR COMPONENTS (cont.)

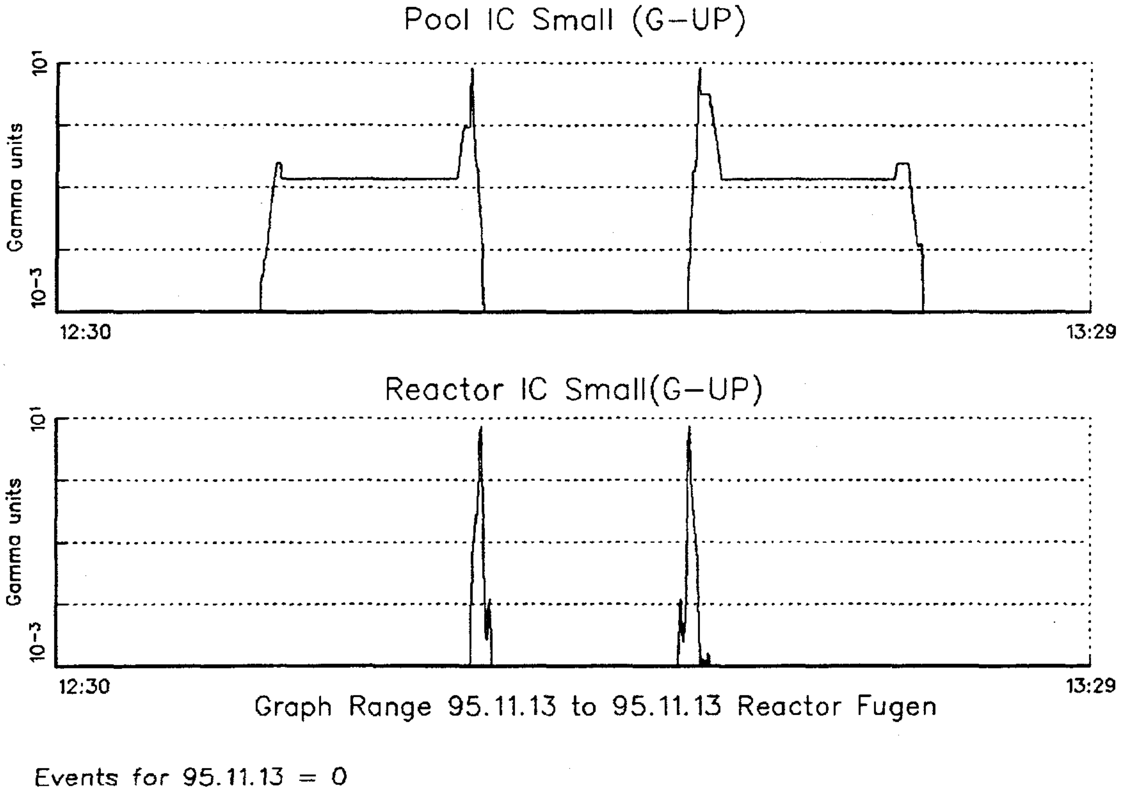

Fig. 23. Double cover-plug transfer (in and out) where the first curve is the small IC (pool) and the bottom curve is the small IC (reactor) (log scale).

signal level for the irradiated fuel. Thus, the cover-plug transfers can be distinguished from fuel assembly transfers by the shape of the pattern, the magnitude of the signal, and the absence of neutrons.

FRESH URANIUM FUEL

The transfer of fresh UOX has a negligible response from both the neutron and gamma emissions. The intrinsic signals from LEU are low and the additional shielding from the water and steel in the transfer chute makes the signal levels too small to detect.

Figure 24 shows the gamma and neutron signal levels for a fresh UOX transfer. The top curve corresponds to the large IC pool and bottom curve corresponds to the ^{3}He-1 signal. The first gamma peak corresponds to the movement of the

FRESH URANIUM FUEL
(cont.)

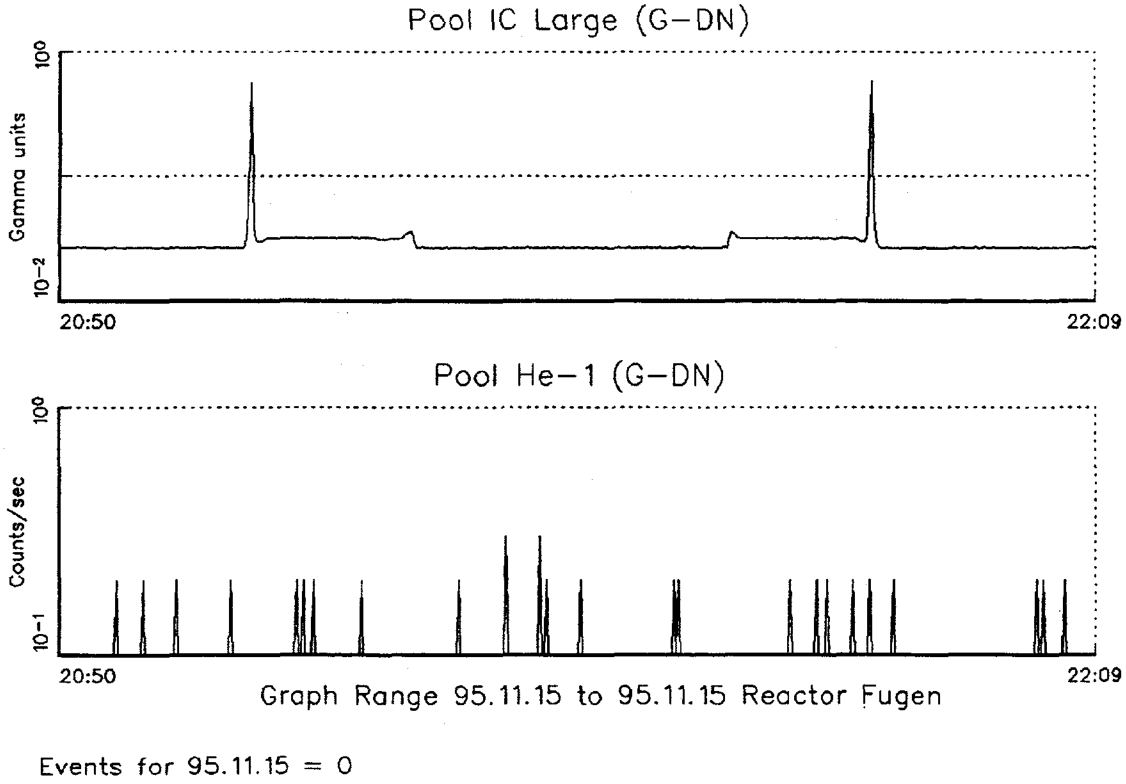

Fig. 24. Fuel assembly transfer for fresh UOX assembly where the top curve is the large IC (pool) and the bottom curve is the ^{3}He-1 (log scale).

empty transfer basket back to the storage pool, and the second peak corresponds to the movement of the loaded transfer basket over the top of detector A going back to the reactor. The fresh UOX transfer takes place at the time of the second peak produced from the transfer basket.

NO FUEL BACKGROUND RATES

The detector background rates when no fuel is being transferred are listed in Table XI. These data correspond to the reload period when the reactor is shut down. Future data will correspond to backgrounds during the operation of the reactor.

NO FUEL BACKGROUND RATES

(cont.)

TABLE XI. Detector Background Rates

Sensor	Zero Power Background (counts/s)
FC-1 (A)	0.1
FC-2(A)	~0.7
He-1(A)	0.1
He-2(A)	~2.5
Lg IC(A)	0.026
Sm IC(A)	0.001
Lg IC(B)	0.002
Sm IC(B)	0.001

The relatively high backgrounds in FC-2 and He-2 are caused by low-activity alpha counts and noise in those two sensors.

MULTIPLE FUEL TRANSFERS

Figure 25 shows the fuel transfer history over an 8-h period that included two irradiated MOX, one irradiated UOX, five transfer containers, and two cover plug transfers. The top curve corresponds to the large IC (pool) data and the bottom curve corresponds to the large FC-1 data. The distinctive patterns between the irradiated fuel transfers and the contaminated equipment transfers are evident in the display. From the data we can calculate the number of transfers, the type of fuel, the direction of transfer, and the speed of transfer. New software to automate the identification of the transfer activity is being written by Los Alamos National Laboratory with support from POTAS. Until this software is completed, the identification is being done manually from the data graphs.

MULTIPLE FUEL TRANSFERS (cont.)

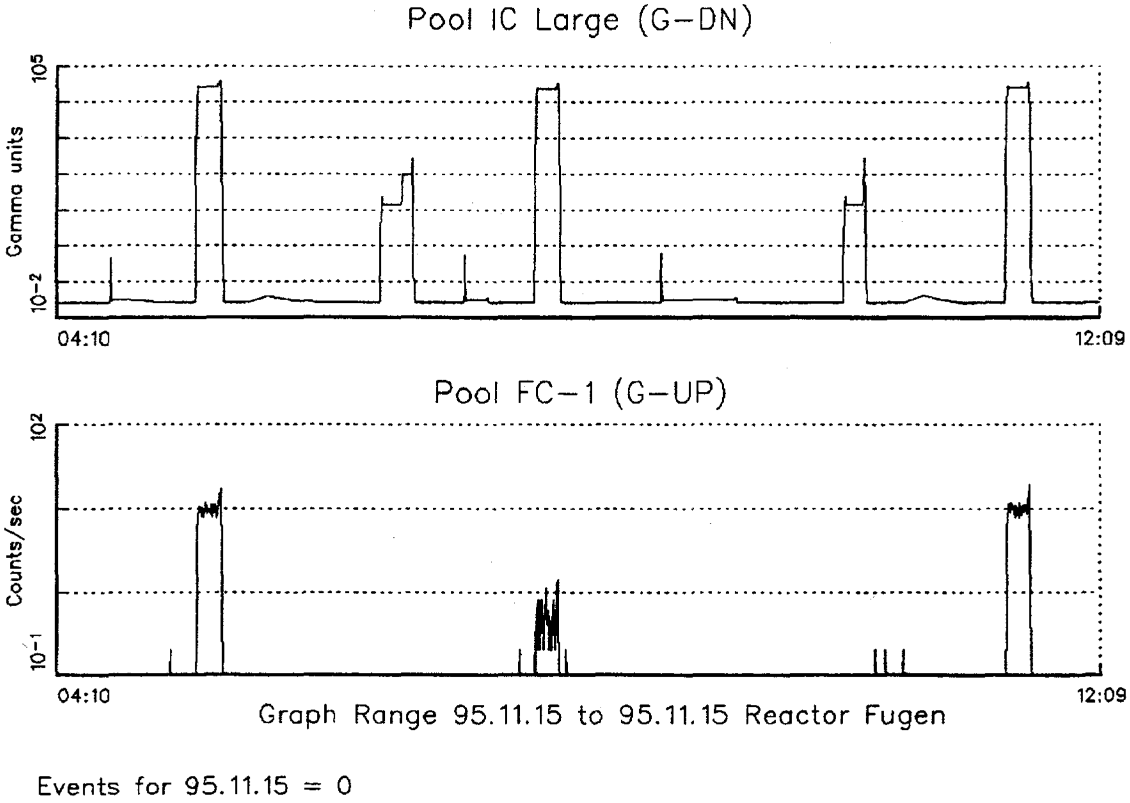

Fig. 25. Fuel assembly transfers over an 8-hour period including two irradiated MOX, one irradiated UOX, and three cover plugs where the top curve corresponds to the large IC (pool) and the bottom curve is the FC-1.

TRANSFER OPERATION

For normal applications of the FUGM system, the fuel is transferred twice a year requiring a 20-40 day halt in reactor operation for the fuel transfers. There might be 30-40 fuel assemblies shuffled during this period. However, each fuel assembly transfer might include four events in the data log because of the fuel plug movement (out and in) and fuel assembly movement (out and in). Thus, the movement of 35 assemblies would result in ~140 signal events being recorded in up to 8 detectors. There typically would be ~840 sensor events for the analysis of a refueling campaign.

REFERENCES

1. J. E. Swansen, "Deadtime Reduction in Thermal Neutron Coincidence Counter," Los Alamos National Laboratory report LA-9936-MS (March 1984).

2. P. M. Rinard and G. E. Bosler, "Safeguarding LWR Spent Fuel with the Fork Detector," Los Alamos National Laboratory report LA-11096-MS (March 1988).

3. H. O. Menlove and J. E. Swansen, "A High-Performance Neutron Time-Correlation Counter," *Nucl. Technol.* **71**, 497-505 (November 1985).